The functional evolution of collembolan Ubx on the regulation of abdominal appendage formation

Yan Liang[1, 2, 3, *], Yun-Xia Luan[1, 4, *]

[1] Key Laboratory of Insect Developmental and Evolutionary Biology, CAS Center for Excellence in Molecular Plant Sciences, Shanghai Institute of Plant Physiology and Ecology, Chinese Academy of Sciences, Shanghai 200032, China

[2] University of Chinese Academy of Sciences, Beijing 100049, China

[3] Current address: Wellcome Sanger Institute, Wellcome Genome Campus, Hinxton, Cambridge CB10 1SA, United Kingdom

[4] Current address: Guangdong Provincial Key Laboratory of Insect Developmental Biology and Applied Technology, Guangzhou Key Laboratory of Insect Development Regulation and Application Research, Institute of Insect Science and Technology, School of Life Sciences, South China Normal University, Guangzhou 510631, China

[*]CORRESPONDENCE TO: yl10@sanger.ac.uk; yxluan@scnu.ac.cn

Abstract

Folsomia candida is a tiny soil-living arthropod belonging to the Collembola, which is an outgroup to Insecta. It resembles insects as having a pair of antennae and three pairs of thorax legs, while it also possesses three abdominal appendages: a ventral tube located in the first abdominal segment (A1), retinaculum in A3 and furca in A4. Collembolan Ubx and AbdA specify abdominal appendages, but they are unable to repress appendage marker gene *Dll*. The genetic basis of collembolan appendage formation and the mechanisms by which Ubx and AbdA regulate *Dll* transcription and appendage development remain unknown. In this study, we analysed the developmental transcriptomes of *F. candida* and identified candidate appendage formation genes, including *Ubx* (*FcUbx*). Expression data revealed the dominance of *Dll* over *Ubx* during the embryonic 3.5 and 4.5 days, suggesting Ubx is deficient in suppressing *Dll* at early appendage formation stages. Furthermore, via electrophoretic mobility shift assays and dual luciferase assays, we found that the binding and repression capacity of FcUbx on *Drosophila Dll* resembles those of the longest isoform of *Drosophila* Ubx (DmUbx_Ib), while the regulatory mechanism of the C-terminus of FcUbx on *Dll* repression is similar to that of crustacean *Artemia franciscana* Ubx (AfUbx), demonstrating that the function of collembolan Ubx is intermediate between that of Insecta and Crustacea. In summary, our study provides novel insights into collembolan appendage formation and sheds light on the functional evolution of Ubx. Additionally, we propose a model that collembolan Ubx regulates abdominal segments in a context-specific manner.

Keywords: Collembola, Arthropoda, appendage formation, RNA-seq, transcriptional regulation, functional evolution

Competing Interests

The authors have declared that no competing interests exist.

Introduction

Extant arthropods are traditionally classified into four major groups: chelicerates, myriapods, crustaceans, and hexapods (including proturans, collembolans, diplurans, and insects) (Budd & Telford, 2009; Giribet et al., 2001; Hughes & Kaufman, 2002b). Throughout their evolution, arthropods gradually reduce abdominal appendages, particularly insects, which entirely lack these appendages in their adult stages (Jockusch & Smith, 2015; Matsuda, 2017). The establishment of a body plan is regulated by a cascade of orchestrated transcription factors during embryogenesis, including maternal effect genes, pair-rule genes, gap genes and Hox genes (Peel et al., 2005). Hox genes encode transcription factors characterized by a helix-turn-helix DNA-binding homeodomain and play pivotal roles in the identification and appendage formation of each segment along the body axis of arthropods (Angelini & Kaufman, 2005a, 2005b; Budd & Telford, 2009; Hughes & Kaufman, 2002a). Typically, Hox genes are organized in a cluster on the chromosome and exhibit both spatial and temporal collinearity in their expression patterns (Durston et al., 2011). *Dll* (*Distal-less*) serves as a marker gene for the appendage primordium in a wide variety of animals (Panganiban et al., 1997), within some groups of pancrustaceans (including crustaceans and hexapods) (Browne & Patel, 2000; Cohen et al., 1991; Jockusch et al., 2004), it acts as a downstream target of Ubx (*Ultrabithorax*) (Buffry et al., 2023; Cohen, 1990; Galant & Carroll, 2002; Gebelein et al., 2002; Palopoli & Patel, 1998; Ronshaugen et al., 2002). In *Drosophila melanogaster*, the Ubx gene generates six isoforms (*Ib*, *Ia*, *IIb*, *IIa*, *IVb*, *IVa*) via alternative splicing events, with variation in the architecture of the linker region between the YPWM motif and homeodomain (HD domain) (Geyer et al., 2015; Passner et al., 1999; Reed et al., 2010). Specifically, the *Ib* isoform (DmUbx_Ib) has the longest linker region, and the *IVa* isoform (DmUbx_IVa) does not contain the linker. Functional assays demonstrated that the longest linker is indispensable for the suppression of *Dll* expression (Gebelein et al., 2002); in addition, the QAQA domains and poly-Ala stretch located at the C-terminus are also crucial for the repression function (Galant & Carroll,

57 2002; Gebelein et al., 2002; Hughes & Kaufman, 2002b; Ronshaugen et al., 2002). In
58 general, these structures facilitate Ubx the ability to bind to the enhancer of *Dll* (Dll304)
59 and consequently suppress the expression of the *Dll* gene (Cohen et al., 1993; Gebelein
60 et al., 2002). In contrast, in branchiopod crustacean *Artemia franciscana*, Ubx (AfUbx)
61 loses its capacity to repress *Dll* expression (Ronshaugen et al., 2002). This functional
62 shift can be attributed to the presence of phosphorylation sites within the C-terminus of
63 AfUbx, which impede its ability to suppress limb development (Galant & Carroll, 2002;
64 Ronshaugen et al., 2002). To date, the evolutionary processes and the molecular
65 mechanism that give rise to the loss of abdominal appendages in adult hexapods remain
66 elusive.
67 Collembola (springtails) is a group of basal hexapods, whose phylogenetic position is
68 intermediated between aquatic crustaceans and terrestrial insects (Gao et al., 2008;
69 Luan et al., 2005; Timmermans et al., 2008). Collembolans bear three distinct types of
70 abdominal appendages (M. T. Fountain & S. P. Hopkin, 2005): the ventral tube (or
71 collophore) in abdominal segment 1 (A1), which is involved in osmoregulation with
72 the external environment; the retinaculum in A3, a structure for holding the springing
73 organ furca in place; and the furca in A4, a robust jumping apparatus (Tully & Potapov,
74 2015). A previous study demonstrated that the collembolan Ubx specifies A1 and AbdA
75 determines A4, and they both regulate the morphological formation of A2 and A3
76 (Konopova & Akam, 2014). Intriguingly, collembolan Ubx, AbdA and *Dll* are
77 concurrently expressed in the collembolan abdomen during the embryonic stage,
78 indicating that collembolan Ubx and AbdA does not repress *Dll* expression in
79 abdominal segments (Palopoli & Patel, 1998). However, the molecular mechanisms of
80 how collembolan Ubx and AbdA interact with *Dll* and thus regulate appendage
81 formation are unclear.
82 To address this question, we conducted a computational analysis of the developmental
83 transcriptomes of Collembola, *F. candida* (Denmark strain), covering embryos and
84 juveniles to adults. Through this analysis, we identified the genes potentially involved

85 in appendage formation during embryogenesis, with *Ubx* being a notable inclusion.
86 Expression data indicated that *Ubx* could not suppress *Dll* in the early appendage
87 formation stages. Furthermore, we investigated the transcriptional regulatory functions
88 of Ubx. Our findings revealed that the binding capacity and repression activity of *F.*
89 *candida* Ubx (FcUbx) on *D. melanogaster Dll* are analogous to those in *D.*
90 *melanogaster* Ubx (DmUbx_Ib) (Galant & Carroll, 2002; Gebelein et al., 2002;
91 Ronshaugen et al., 2002); and the regulatory mode and site(s) in the C-terminus of
92 FcUbx resemble those of Ubx in the branchiopod crustacean *A. franciscana* (AfUbx)
93 (Galant & Carroll, 2002; Ronshaugen et al., 2002). Based on these data, we depicted a
94 molecular functional evolutionary model of Ubx from crustaceans to basal hexapods to
95 insects in the broad scope of panarthropods and proposed that the collembolan Ubx
96 might exert its repression function in distinct abdominal segments in a context-specific
97 manner.
98

99 **Materials and methods**

100 **Sample collection and transcriptome sequencing**

101 First, *F. candida* (Denmark strain) was synchronized for three generations: some adult
102 individuals (F_0 generation) were transferred to a new Petri dish (10 cm), a container
103 with a layer of a mixture of plaster of Paris and activated charcoal at a ratio of 9:1 by
104 weight (Krogh, 2009). After 24 hours of oviposition, the eggs (F_1 generation) were
105 subsequently transferred to a new Petri dish for one month of culture to reach sexual
106 maturity. The procedure was repeated twice to obtain synchronized adults of the F_3
107 generation. Approximately 300 adults of the F_3 generation were then transferred to three
108 new Petri dishes for 24 hours of oviposition, and all eggs were transferred to a new
109 culture dish. Next, all eggs laid by the F_3 generation were collected and transferred to
110 new culture dishes (5 cm) every 24 hours, except on the last day, when eggs were
111 collected at 12 hours after the adults had been transferred.
112 After 51 days of collection and culture, we obtained 51 samples ranging from day 0.5

113 to day 50.5. Fifteen developmental samples, including eggs (from days 0.5 to 9.5),
114 juveniles (days 12.5, 19.5 and 28.5), and adults (days 31.5 and 45.5), were chosen for
115 transcriptome sequencing. RNA was prepared and extracted separately from 15 samples
116 by using a miRNeasy mini kit (QIAGEN, Germany) according to the manufacturer's
117 instructions. The transcriptomes were sequenced on the BGISEQ-500 platform by BGI
118 (Yuzuki, 2015) (Shenzhen, China). All of the raw reads had been published (BioProject
119 PRJNA433725) (Liang et al., 2019).
120

121 **Transcriptome analysis and gene annotation**

122 The reads mapping and differential gene expression analysis were identical to the
123 previous study (Liang et al., 2019). The genome we used was non-chromosome-level
124 genomic data from the published *F. candida* genome (Luan et al., 2023). The genome
125 index was built using bowtie2 (Langmead & Salzberg, 2012), and the reads were
126 mapped using tophat2 (Kim et al., 2013) The transcript abundance (RPKM) was
127 estimated using cufflinks (Trapnell et al., 2012), with the gene annotation file from the
128 whole genome. Gene Ontology (GO) annotations were accomplished by running
129 BLAST2GO (Conesa et al., 2005) against the UniProt database (UniProt release
130 2018_02) (Bairoch et al., 2005). The expression profile was obtained from the data
131 matrix representing the expression abundance (RPKM, reads per kilobase of transcript
132 per million fragments mapped) from 15 transcriptomes. The distribution of gene
133 expression was visualized as Ridgeline Plots in 'ggplot2' (Wickham, 2016).
134 Additionally, to explore the relationships among developmental stages, we employed
135 several analyses. Principal component analysis was conducted using the "prcomp"
136 function, while Pearson correlation analysis was executed using the "cor" function in
137 R. For hierarchical clustering analysis, we first scaled the dataset using the "Euclidean"
138 method and then applied the "hclust" function with the "ward.D2" method. Data
139 visualization was achieved using "ggplot2" and "pheatmap" (Kolde, 2012) in RStudio
140 (2023.3.0.386) (RStudio, 2020).

141

142 **Mining of genes involved in appendage formation**

143 To identify genes associated with the appendages formation from time-series bulk
144 RNA-seq data, we employed the Short Time-series Expression Miner (STEM)
145 approach (Ernst & Bar-Joseph, 2006; Ernst et al., 2005), which attempts to assign genes
146 to previously defined temporal trajectory/development (Bar-Joseph et al., 2012).
147 Through the embryonic observation, PCA analysis, and hierarchical clustering, we
148 selected four key time points: day 1.5 (E_1.5d, blastula, no appendages), day 3.5
149 (E_3.5d, early stage of appendage formation), day 5.5 (E_5.5d, mid-stage of appendage
150 formation) and day 7.5 (E_7.5d, mature stage of appendage formation) for mining genes
151 were involved in appendage formation. STEM software was used to classify all the
152 clusters according to the abundance of gene expression. Subsequently, genes in the
153 clusters that were supposed to correlate with appendage formation were sorted out and
154 then annotated by Blast2GO software (Conesa et al., 2005).

155

156 **Expression profiling of Hox genes and *Dll* in *D. melanogaster* and *F. candida***

157 The gene expression profile of *D. melanogaster* was downloaded from flybase
158 (http://ftp.flybase.org/releases/current/precomputed_files/genes/gene_rpkm_matrix_fb
159 _2023_05.tsv.gz) (Brown et al., 2014). The expression values of Hox genes and *Dll*
160 were subset from the expression profile of *D. melanogaster* and *F. candida*. Notably,
161 the *Ubx* in *F. candida* was fragmented into five transcripts (XLOC_011518,
162 XLOC_011661, XLOC_011777, XLOC_011778 and XLOC_011779) (Supplementary
163 Data 1). To calculate the expression of *Ubx*, we computed and accumulated the RPKM
164 of those transcripts. The normalization of gene expression was applied in two
165 approaches. Normalized RPKM, the original RPKM was normalized by comparing the
166 minimum and maximum of each gene throughout the embryonic stages to elucidate the
167 expression pattern and the lowest and highest expression stage of a gene. Z-score, the
168 original RPKM was normalized by the z-scale in R (RStudio, 2020), which can reflect

169 the expression pattern of all the selected genes.

170

171 **Mining of genes correlated with *Ubx* from transcriptomes**

172 To predict the putative function or the underlying regulation of Ubx, based on the gene
173 expression profile, we used the Spearman correlation algorithm (Spearman correlation
174 coefficient $r > 0.9$, $p < 0.01$) to mine genes coexpressed with *Ubx* during embryogenesis.
175 The coexpressed genes were extracted and then annotated by Blast2GO of gene
176 ontology terms (GO terms) and KEGG pathway annotation (Conesa et al., 2005;
177 Kanehisa & Goto, 2000).

178

179 **Acquisition of *Ubx*, *Exd* and *Hth* sequences**

180 The complete sequences of two isoforms of *Ubx* in *F. candida* (Collembola) and the
181 partial sequences from *Sinentomon erythranum* (Protura) and *Campodea augens*
182 (Diplura) were cloned by degenerate PCR from the homeodomain, further obtained by
183 5' RACE and 3' RACE. Specifically, two isoforms of FcUbx were validated by using
184 exon-intron and exon-exon junction PCR with overlapping primers spanning the linker
185 region. *Exd* and *Hth* were identified via BLAST (Altschul et al., 1990; McGinnis &
186 Madden, 2004) from transcriptomes and further validated by PCR cloning. All
187 sequences were submitted to NCBI (OR593736, OR593737, OR593738, OR593739,
188 OR604006, OR604007). The sequences of Panarthropod Ubx were aligned by MAFFT
189 (Rozewicki et al., 2019), and the gaps were removed manually. The multiple sequence
190 alignment was visualized in Jalview (Waterhouse et al., 2009).

191

192 **Protein expression and purification**

193 The N-terminus truncated collembolan proteins, FcU1, FcU2, Exd and Hth used for
194 protein expression were constructed in the pGEX-4t-1 plasmid (GST-tag inserted) and
195 transformed into *E. coli* competent cells (BL21 strain). Protein expression was first

196 started from 500 mL of Luria–Bertani (LB) medium (pH = 7) cultured at 37 °C at 220
197 rpm. Until it reached the exponential growth phase (OD600 = 0.8~1.0), isopropyl β-D-
198 1-thiogalactopyranoside (IPTG) was added (0.1 mM) to 2 L of LB medium. The whole
199 culture was then subjected to low-temperature induction of protein expression at 16 °C
200 and 220 rpm for 12 hours. All the GST-tagged proteins were purified in native
201 conditions according to the manufacturer's instructions (Sangon Biotech, Shanghai,
202 China). All proteins were quantitated by comparing them to a set of bovine serum
203 albumin (BSA) concentration gradients: 750, 500, 250, 125, 100, 75, 50, 25, and 0 ng/μl
204 by Coomassie blue staining and further confirmed by anti-GST western blotting.
205

206 **Electrophoretic mobility shift assays (EMSAs)**

207 We identified a putative FcDll Element (PFE) in *F. candida* through a search within the
208 approximately 4000 bp intergenic genomic region upstream of the first exon of the
209 collembolan *Dll* gene. This search utilized the Hox binding consensus sequence (5'-
210 TATA-3') (Berger et al., 2008; Ekker et al., 1991; Noyes et al., 2008) and the Exd
211 binding consensus sequence (5'-TGAT-3') (Ryoo et al., 1999; Slattery et al., 2011).
212 For EMSAs, the DMXR element (Gebelein et al., 2002; Gebelein et al., 2004), a
213 repression regulatory element of *Dll* (Dll304) in *D. melanogaster*, and the putative
214 regulatory element of *Dll* in *F. candida* (Putative FcDll Element, PFE) were utilized as
215 a DNA probe in each assay separately. The probe was first synthesized as two separate
216 primers (forward and reverse strands), which were tagged with Cy5 at the 5' end. The
217 primers were diluted to a concentration of 1 μM. Subsequently, 50 μl of each primer
218 was mixed and incubated at 95 °C and then cooled to room temperature. The primers
219 were annealed, resulting in the formation of double-stranded DNA probes. 20 ng of
220 DNA probe was used in each EMSA, and the amount of protein used in each EMSA
221 was 10 pmol of GST, 0.2, 1, and 1.5 pmol of FcU1, 0.4, 2, and 3 pmol of FcU2 and 1
222 pmol of Exd and Hth. The procedures for electrophoretic mobility shift assays (EMSAs)
223 were adjusted and visualized according to the protocol (He et al., 2016). The 20 μl

224 EMSA solution: 5× EMSA buffer: Tris (0.1 M), glycerol (25%), and BSA (0.2 mg/ml).
225 2.5 M $MgCl_2$, 1 M DTT, double-distilled water, poly(dI-dC), protein, and Cy5-labelled
226 DNA probe. The reaction was incubated for 25 minutes at 25 °C. The 12% non-
227 denaturing polyacrylamide gel contained double-distilled water, 5× TBE buffer, 50%
228 glycerol, polyacrylamide (the monomer: dimer ratio was 80:1), 10% ammonium
229 persulfate, and tetramethyl ethylenediamine (TEMED). Electrophoresis was carried out
230 on ice, with the blank gel pre-electrophoresed at 120 V for 1 hour. Subsequently, 20 μl
231 of the reaction mixture was loaded into each vial of the gel, and the samples were run
232 at 150 V for 1-1.5 hours. For reaction visualization, the entire gel with the glass
233 container was scanned directly with the A Starion FLA-900 phosphorimager (Fujifilm,
234 Japan).
235

236 ***Drosophila* S2 cell transfection and dual luciferase reporter assays**

237 The complete sequences of *D. melanogaster* Ubx (DmUbx_Ib, DmUbx_IVa) and
238 collembolan Ubx (FcU1, FcU2), the truncated collembolan Ubx (FcU1/△C, FcU2/△C)
239 and chimeric Ubx of *Drosophila* and collembolan (Dm/Fc_L, Dm/Fc_C) were cloned
240 into the pAC5.1 expression vector. To test the repression on DMXR, this regulatory
241 sequence was constructed into a pGL3-promoter vector (Promega), which contains the
242 SV40 enhancer and firefly luciferase. Transfection experiments were carried out using
243 the Qiagen Effectene reagent (Qiagen, Germany), according to the manufacturer's
244 protocol. Initially, *Drosophila* S2 cells were cultured in Schneider's *Drosophila* medium
245 (Sigma–Aldrich, USA) supplemented with 10% fetal bovine serum (HyClone, USA).
246 After 24 hours, the cells were aliquoted into 48-well plates at 150 μl per well. After 12
247 hours, 50 μl of DNA-enhancer mixture, containing 1.2 μl of enhancer (the reagent from
248 the Effectene reagent kit), 0.075 μg of pGL3-promoter vector, 0.075 μg of pAC5.1
249 vector, and 0.2 μl of the Renilla fluorescent vector (pRL) were added to the mixture,
250 followed by an 8-minute incubation. Then, 4 μl of Effectene and 200 μl of cell culture
251 medium were added, and the transfected cells were cultured for 48 h in a 27 °C

252 incubator. Each protein vector was set with technical triplicates.

253 The Dual luciferase reporter assay kit (Promega, USA) was used to measure the reporter
254 gene expression, and the luciferase activities were detected by a Modulus^{TM} Microplate
255 Luminometer (Turner BioSystems, USA). The repression activity of each protein is
256 represented by the average ratio of Firefly: Renilla luciferase activity. To estimate the
257 relative repression of the proteins on the DMXR, we compared the repression activity
258 of each sample with that of DmUbx_Ib. For pairwise comparisons, we performed
259 Student's t-test in R (RStudio, 2020).

260

261 **Results**

262 **Development and time-course transcriptomes of *F. candida***

263 The embryos of *F. candida* (Denmark strain) took approximately 10 days to reach the
264 juvenile stage when incubated at 21 °C (Michelle T. Fountain & Steve P. Hopkin, 2005).
265 Referring to the observation of the embryonic developmental stages in *F. candida*
266 (Shanghai strain) (Gao et al., 2006), the samples selected for sequencing are illustrated
267 in Figure 1A. The embryos in the 0-0.5 day (E_0.5d) predominantly ranged from the 4-
268 cell stage to the blastula stage. By 1.5 days, most embryos had progressed in the gastrula
269 stage. In 2.5 days, the initial phase of tissue differentiation stage, characterized by the
270 segmentation and formation of appendage primordia. At 3.5 days, the antenna and
271 thorax appendages started segmentation and elongation; the furca was observed by 4
272 days (Gao et al., 2006). During the period of 4.5 to 6.5 days, the middle phase of the
273 tissue development stage progressed, accompanied by the growth and maturation of
274 appendages. From 7.5 to 8.5 days, in the late phase of tissue differentiation, the
275 appendages were fully formed, and the animals were preparing for hatching. Finally, at
276 9.5 days, the animals were actively moving within the eggshell, and some individuals
277 had already hatched. Typically, it took these juveniles one month to reach sexual
278 maturity as adults (Figure 1A, 1C).

279 The analysis of developmental transcriptomes recaptured the expression of a total of

280 25,803 genes throughout the developmental process (Figure 1B, Supplementary Data
281 1). Transcriptomic analyses elucidated that the relationships of all the developmental
282 samples were consistent with the observation of development (Figure 1A, 1D, 1E, 1F).
283 In general, all the post-hatching samples (juveniles and adults) clustered together,
284 demonstrating that the hatching event acted as a critical developmental transitional
285 event (Figure 1D, 1E, 1F). The embryonic samples were grouped separately: in the
286 early stages E_0.5d and E_1.5d, no appendages were observed, and these two stages
287 were grouped; the embryonic stages E_2.5d and E_3.5d, particularly marked by the
288 segmentation and formation of appendage primordia, were clustered; and the period
289 spanning from E_4.5d to E_9.5d, deemed the development of appendages, formed a
290 distinct group. Specifically, E_4.5d to E_5.5d represent the mid-phase of appendage
291 formation, and E_6.5d to E_9.5d were identified as the maturation of appendage
292 formation (Figure 1D, 1E, 1F).
293

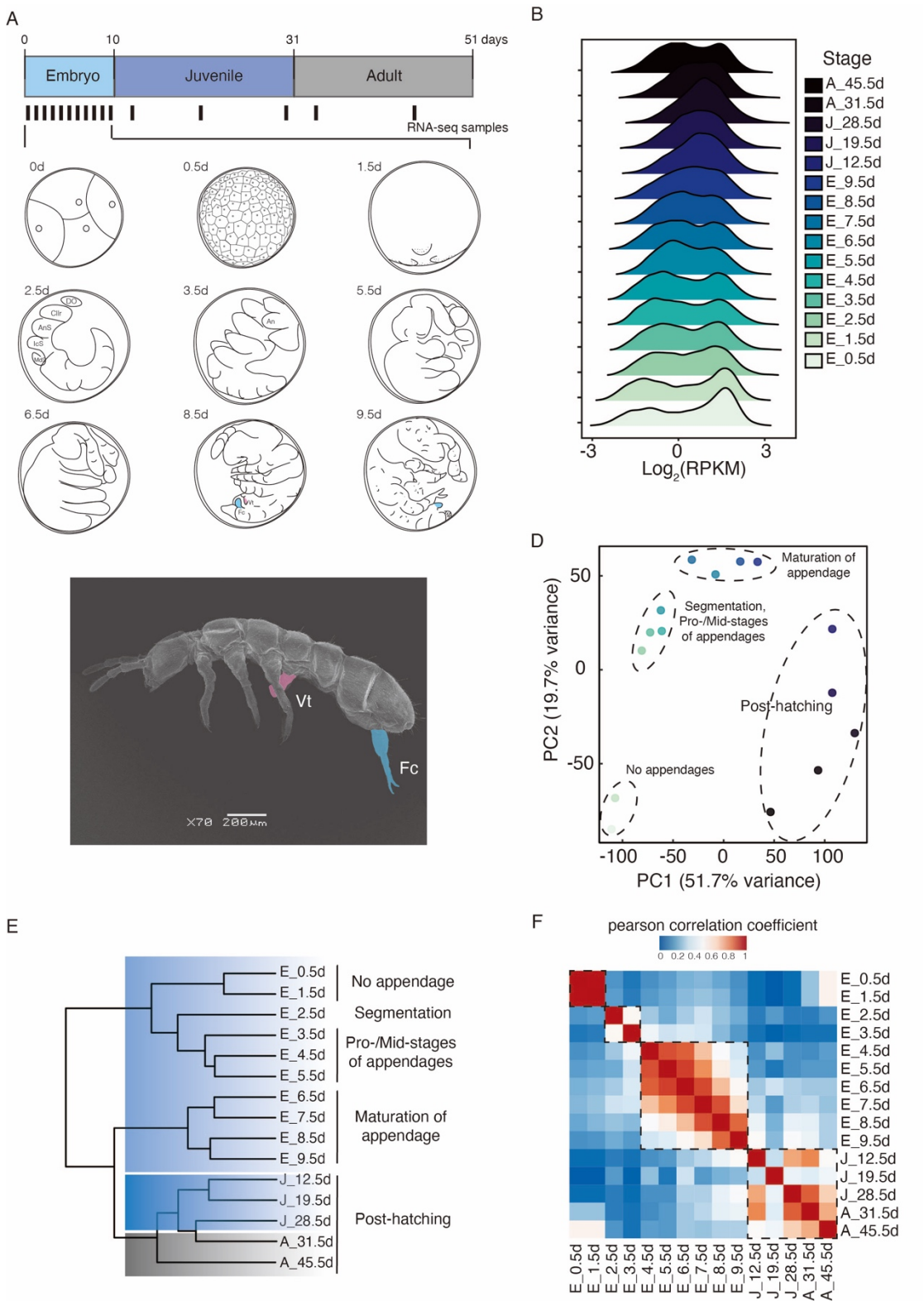
A
0
10
31
51 days
Embryo
Juvenile
Adult
RNA-seq samples
0d
0.5d
1.5d
2.5d
3.5d
5.5d
6.5d
8.5d
9.5d
B
Stage
A_45.5d
A_31.5d
J_28.5d
J_19.5d
J_12.5d
E_9.5d
E_8.5d
E_7.5d
E_6.5d
E_5.5d
E_4.5d
E_3.5d
E_2.5d
E_1.5d
E_0.5d
-3
0
3
Log2(RPKM)
Vt
Fc
D
Maturation of appendage
Segmentation, Pro-/Mid-stages of appendages
Post-hatching
No appendages
PC2 (19.7% variance)
PC1 (51.7% variance)
E
No appendage
Segmentation
Pro-/Mid-stages of appendages
Maturation of appendage
Post-hatching
F
pearson correlation coefficient
0 0.2 0.4 0.6 0.8 1

294

295

296 **Figure 1 Analysis of developmental transcriptomes of *F. candida*.**

297 **A**. Schematic of samples for developmental transcriptome sequencing and the
298 observation of embryonic development. Whole-animal collections were made from
299 embryos (blue), juveniles (grey blue) and adults (grey). The bars indicate that different
300 developmental samples were collected. 0d (d, days after oviposition): 4-cell stage; 0.5d:
301 blastula stage; 1.5d: gastrula stage; 2.5d: Initial phase of tissue differentiation stage;
302 3.5-6.5d: middle phase of tissue differentiation stage; 7.5-8.5d: Late phase of tissue
303 differentiation stage; 9.5d: prehatching stage. An: antenna; AnS: antenna segment; Cllr:
304 clypeolabrum; DO: dorsal organ; Fc: furca (in blue colour); IcS: intercalary segment;
305 MdS: mandibular segment; Vt: ventral tube (in pink colour). **B**. Distribution of gene
306 expression of 25,038 genes from 15 developmental transcriptomes. RPKM, reads per
307 kilobase per million, normalizes the raw count by transcript length and sequencing
308 depth. **C**. Scanning electron microscopy (SEM) of the whole animal of adult *F. candida*.
309 Vt: ventral tube (shade in pink colour), Fc: furca (shade in blue colour). **D**. Principal
310 component analysis of the developmental transcriptomes. The dashed ellipses indicate
311 the stages of appendage development. **E**. Simplified hierarchical clustering of all
312 developmental transcriptomes. The stages of appendage development are shown on the
313 right. **F**. Heatmap of the Pearson correlation coefficient of all the samples; the dashed
314 rectangles indicate the relationship of samples.
315

316 **Mining of genes related to appendage development in Collembola**

317 Springtails bear three pairs of thoracic legs and appendages in the abdomen (Figure 1C).
318 These abdominal appendages, however, exhibit distinct morphological characteristics
319 from each other (Figure 1C). To identify genes associated with the establishment of
320 appendages, especially the abdominal appendages, we conducted a Short Time-series
321 Expression Miner analysis (STEM analysis) (Ernst & Bar-Joseph, 2006), which would
322 assign genes to one of several previously defined developmental trajectories (Bar-
323 Joseph et al., 2012). Based on the embryonic observation (Figure 1A) and
324 transcriptomic analyses (Figure 1D, 1E, 1F), we deem the formation of appendages as
325 four stages for our analysis: E_1.5d, corresponding to the blastula stage without any
326 appendage structure; E_3.5d, representing the early stage of appendage development,
327 marked by the emergence of the appendage primordia; E_5.5d, indicating middle stage
328 of appendage development; and E_7.5d, the late stage of appendage development.

329 The number of expressed genes (RPKM > 0) in these four stages was 15,131, 18,693,
330 19,114 and 20,841 genes, respectively (Figure 2A, Supplementary Data 1, 2). The
331 STEM analysis automatically categorized these genes into 50 profiles, among which 12
332 clusters were significantly statistically enriched (permutation test, $p < 0.001$). Per the
333 morphological observations (Figure 1A) and the developmental trend we defined, the
334 emergence of appendages is characterized by gradual development, with the transition
335 of gene expression levels from low to high (Figure 2B). Cluster 42, which reflected this
336 trend, was selected for further investigation (Figure 2C). Cluster 42 contained a total of
337 865 genes and 2,318 transcripts, of which 1,229 were annotated by Blast2GO
338 (Supplementary Data 3). These genes were annotated as 10 biological processes of GO
339 terms (Figure 2D) and involved in 32 KEGG pathways (Supplementary Data 3). In
340 particular, 66 transcripts were associated with the developmental process, of which 36
341 transcripts were annotated, and 18 genes are the morphogenesis and appendages-related
342 genes (Table 1, Supplementary Data 3). These genes constitute a set of conventional
343 hierarchical developmental genes (Peel et al., 2005), including the body patterning gene

Notch (de Celis et al., 1998; Kurata et al., 2000; O'Day, 2006; Rauskolb & Irvine, 1999) and Engrailed (Brower, 1986; van de Heuvel et al., 1993); limb proximal-distal axis formation genes *Exd, Hth* (Wu & Cohen, 1999); and the body plan "selector genes", the Hox genes *Ubx*, *Antp*, and *Scr* (Weatherbee & Carroll, 1999). This cluster also comprised genes relevant to muscle and actin function, *e.g.*, *MYO1E* (*Myo61F*, orthologous in *D. melanogaster*) is an unconventional myosin-like protein (McIntosh & Ostap, 2016), *Lhx1* (*Lim1,* orthologous in *D. melanogaster*), which regulates tarsal segments (Natori et al., 2012); and *FBN2* (*CG7526*, orthologous in *D. melanogaster*) involves in fibrosis (Mead et al., 2022).

In summary, STEM analysis effectively identified several genes closely associated with appendage formation, thus validating the predefined stages utilized for identifying appendage formation genes.

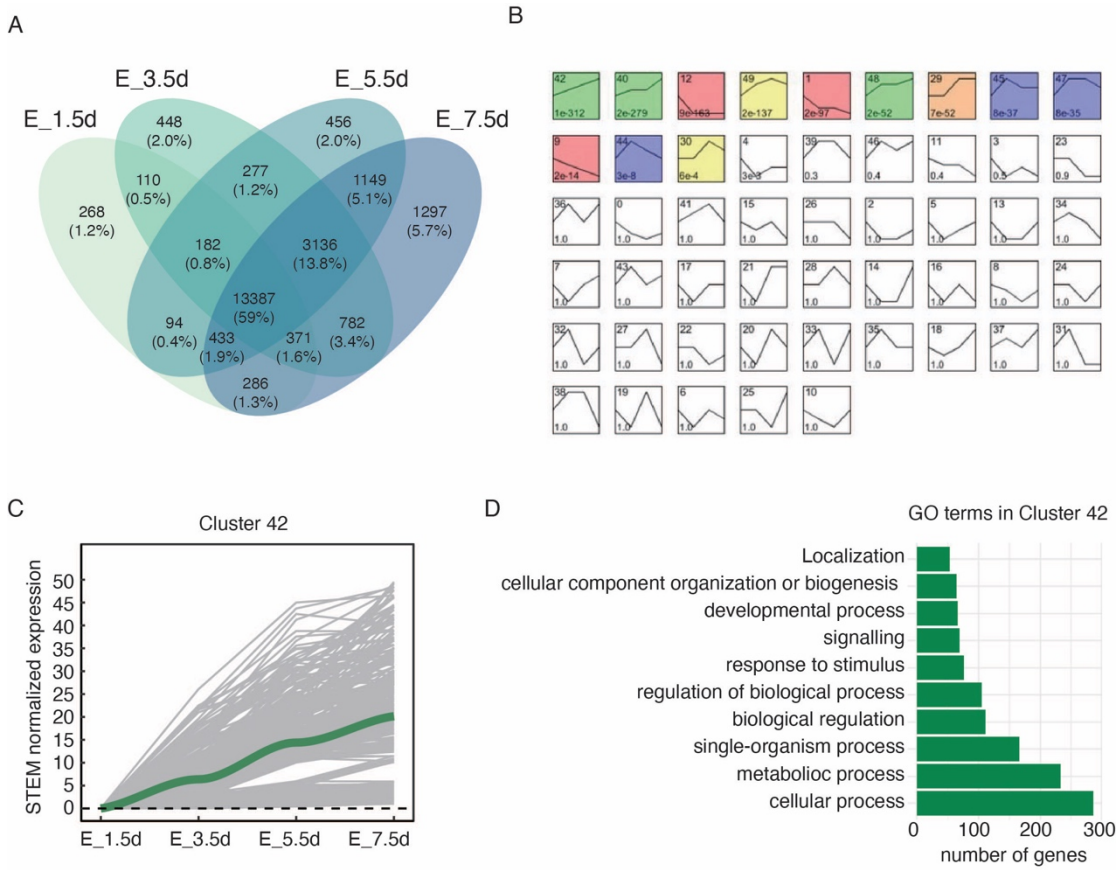

Figure 2 Identification of genes involved in appendage formation.

A. Venn diagram illustrating the number and percentage of expressed genes of each intersection among the four appendage formation stages. **B.** A screenshot of different gene expression profiles identified by short time-series expression miner (STEM) analysis. The number of each profile is shown at the upper left in the square. The coloured profiles indicated that genes were clustered significantly (permutation test, $p < 0.001$). **C.** The STEM normalized expression of Cluster 42. Values higher than 50 were excluded. **D.** Annotated GO terms of Cluster 42.

367 **Table 1** Genes classified in morphogenesis by BLAST2GO from Cluster 42.

Gene_ID	Gene_symbol	Orthologous in *D. melanogaster*	Molecular function
XLOC_013891	FBN2	CG7526	embryonic limb morphogenesis
XLOC_001350	Exd	Exd	somatic muscle development
XLOC_002645	Actin	Actin	muscle contraction
XLOC_017923	BMI1	Psc/Su(z)2	segment specification
XLOC_019142	GATA-3	pnr/grn	anatomical structure morphogenesis
XLOC_016846	Wnt16	Wnt5/ Wnt4	Wnt signaling pathway
XLOC_022735	En	engrailed	trunk segmentation
XLOC_011518	Ubx	Ubx	specification of segmental identity
XLOC_011519	Antp	Antp	specification of segmental identity
XLOC_015540	ROR1	Ror	inner ear development
XLOC_005027	FOX	FoxF	anatomical structure morphogenesis
XLOC_013406	MYO1E	Myo61F/ Myo31DF/ CG15831	microtubule-based movement
XLOC_016945	Notch	Notch	anterior/posterior pattern specification
XLOC_011524	Scr	Scr	specification of segmental identity
XLOC_009469	Ski	CG7233/Snoo	embryonic limb morphogenesis
XLOC_019633	Hth	Hth	segmentation
XLOC_007689	LARGE2	No Data	muscle cell cellular homeostasis
XLOC_016637	Lhx1	Lim1	anatomical structure morphogenesis

368

369 ***Dominance* of *Dll* over *Ubx* during appendage formation in *F. candida***

370 In general, the Hox cluster is characterized by spatial (Figure 3A) and temporal
371 collinearity (Monteiro & Ferrier, 2006). However, previously reported genome
372 assemblies of *F. candida* (Faddeeva-Vakhrusheva et al., 2017; Luan et al., 2023) reveal
373 that *Scr*, *Antp* and *Ubx* inserted into the anterior region of the Hox complex, indicating
374 a lack of spatial collinearity (Figure 3A) (Faddeeva-Vakhrusheva et al., 2017). Our
375 expression analysis of Hox genes in *D. melanogaster* also reveals a lack of temporal
376 collinearity (Figure 3B), consistent with the previous study (Gaunt, 2015). Similarly,
377 the Hox genes in *F. candida* do not display temporal collinearity (Figure 3D). For
378 instance, the *pb* gene was transcribed at E_3.5d, occurring later than *Dfd* and *Scr*, and
379 the most posterior gene *AbdB* was highly expressed at the early stage of E_4.5d;
380 Notably, *Ubx* specifically displayed the highest expression levels at the appendage
381 maturation stage E_7.5d.

382 In *D. melanogaster*, Ubx acts as a *Dll* repressor during embryogenesis in the abdominal
383 segments (Gebelein et al., 2002). The transcriptomic expression data demonstraes that
384 Drosophila *Ubx* exhibited higher expression levels than *Dll* (Figure 3F) during
385 embryogenesis, suggesting its role in repressing *Dll*. Conversely, in *F. candida*, *Dll*
386 predominated over *Ubx* during the E_3.5d and E_4.5d stages (Figure 3G), indicating
387 that FcUbx may not repress *Dll* during the appendage formation stage. However, from
388 the E_5.5d stage onward, *Ubx* expression surpassed that of *Dll*, indicating its potential
389 to regulate or suppress *Dll* during the appendage maturation.

390

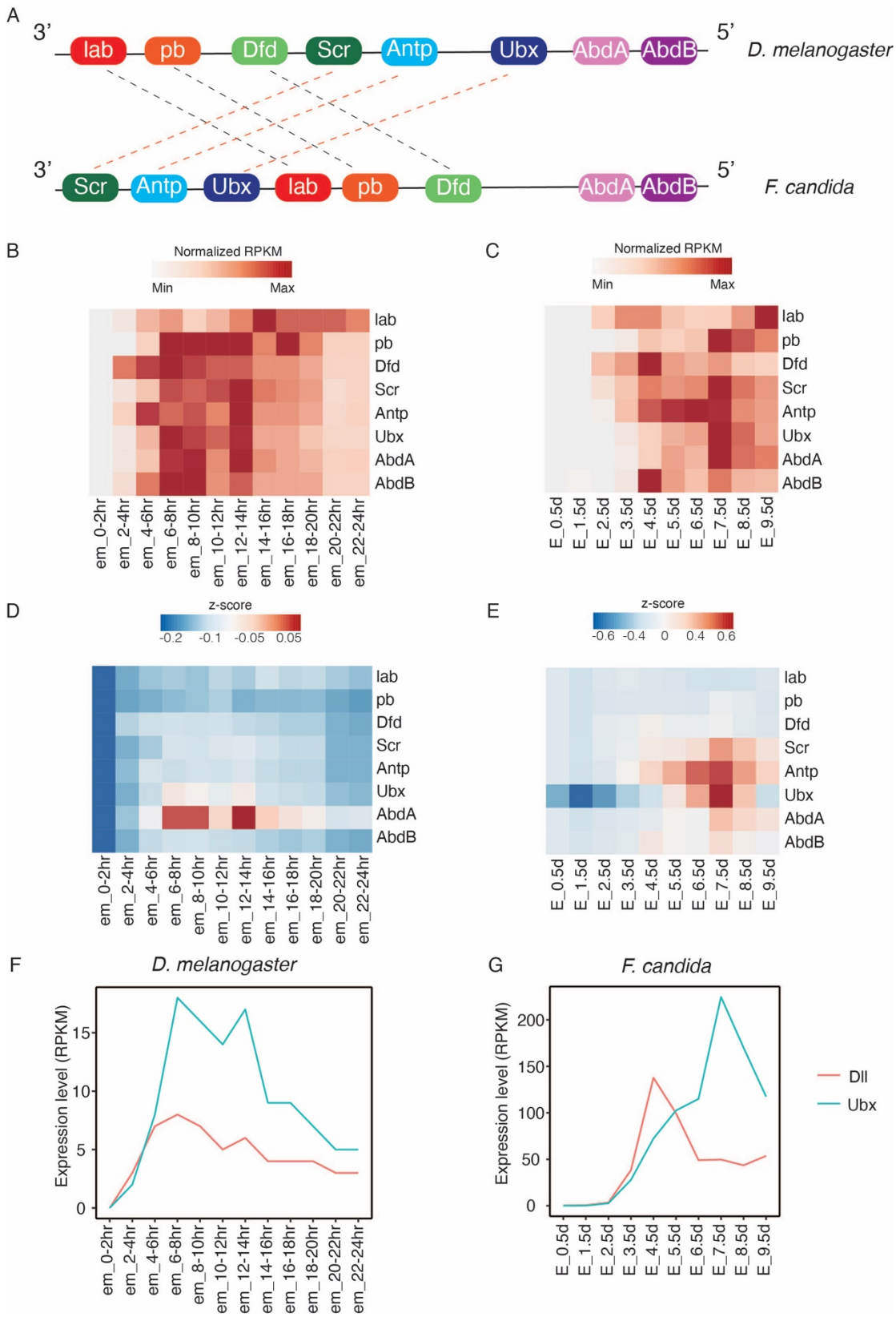
A
3'
lab
pb
Dfd
Scr
Antp
Ubx
AbdA
AbdB
5'
D. melanogaster
3'
Scr
Antp
Ubx
lab
pb
Dfd
AbdA
AbdB
5'
F. candida
B
Normalized RPKM
Min
Max
lab
pb
Dfd
Scr
Antp
Ubx
AbdA
AbdB
em_0-2hr
em_2-4hr
em_4-6hr
em_6-8hr
em_8-10hr
em_10-12hr
em_12-14hr
em_14-16hr
em_16-18hr
em_18-20hr
em_20-22hr
em_22-24hr
C
Normalized RPKM
Min
Max
E_0.5d
E_1.5d
E_2.5d
E_3.5d
E_4.5d
E_5.5d
E_6.5d
E_7.5d
E_8.5d
E_9.5d
D
z-score
-0.2
-0.1
-0.05
0.05
E
z-score
-0.6
-0.4
0
0.4
0.6
F
D. melanogaster
Expression level (RPKM)
0
5
10
15
G
F. candida
Expression level (RPKM)
0
50
100
150
200
Dll
Ubx

391

392 **Figure 3 Comparison of the Hox cluster and *Dll* gene expression between *D.***
393 ***melanogaster* and *F. candida*.**

394 **A.** Genomic architecture of the Hox cluster in *D. melanogaster* (Refined from Pearson,
395 et al. 2005) and *F. candida* (Refined from Faddeeva-Vakhrusheva, et al. 2017). The
396 distances between genes were not scaled in proportion to the original genomic distance.
397 Dashed lines indicate that the Hox genes are rearranged. **B, C, D, E, F, G.** Expression
398 profiles of Hox genes and *Dll* in *D. melanogaster* **(B, D, F)** and *F. candida* **(C, E, G)**.
399 Normalized RPKM, the RPKM were normalized by the minimum and maximum
400 expression value of each gene throughout embryonic stages. Z-score, the RPKM values
401 were normalized by z-scale.
402

403 **Collembolan Ubx can bind to Hox/Exd/Hth DNA binding motifs**

404 Ubx regulates *Dll* through DNA binding and transcriptional repression (Galant &
405 Carroll, 2002; Gebelein et al., 2002; Grenier & Carroll, 2000; Ronshaugen et al., 2002).
406 However, the mechanism of collembolan Ubx interacting with *Dll* remains unclear. To
407 address this, we first obtained two complete isoforms of *Ubx* from *F. candida*, which
408 are produced by alternative splicing and vary at the linker region (FcUbx, isoform 1,
409 FcU1 with a linker of GQSYL; isoform 2, FcU2 without a linker) (Supplementary Data
410 4); and investigated their binding capacity and repression activity through *in vitro* and
411 *in vivo* assays.

412 We conducted the electrical mobile shift assays (EMSAs) to examine the binding
413 capacity of collembolan Ubx on an exogenous *Dll* element, the *Dll* regulatory element
414 of *D. melanogaster* (DMXR, the repression element on Dll304) (Gebelein et al., 2004)
415 (Figure 4A). The proteins of two isoforms of collembolan Ubx (FcUbx1, FcUbx2) can
416 readily bind to DMXR, demonstrating that FcUbxs exhibit binding capability and that
417 their linker region does not affect this binding ability (Figure 4B). Furthermore, the
418 dimer Exd/Hth stimulates Ubx binding to DNA and forms Ubx/Exd/Hth trimeric
419 protein complexes (Figure 4B), thereby demonstrating the ability of collembolan
420 Ubx/Exd/Hth complexes to bind exogenous *Dll* in vitro.

421 To test the binding capacity of collembolan Ubx/Exd/Hth complex on its *Dll* DNA, we
422 searched for *Dll* regulatory elements within approximately 4000 bp of the intergenic
423 genomic region upstream from the first exon of *Dll* (Supplementary Data 6). We
424 identified a binding motif containing both Hox/Exd binding sites and referred to this
425 element as the Putative FcDll Element (PFE) (Figure 4A, Supplementary Data 6). The
426 EMSAs show that FcUbx1 and FcUbx2 cooperatively bind with Exd and Hth on this
427 DNA element (Figure 4C), providing additional evidence that collembolan Ubx is
428 proficient in binding DNA defined as the endogenous Hox/Exd binding element.
429 Nonetheless, owing to the absence of practical genetics tools in collembolans, the
430 validation of whether this DNA element serves as the regulatory region of *Dll* in

431 collembolans remains unattainable.

432 We conclude that the collembolan regulatory trimeric complex Ubx/Exd/Hth can
433 effectively bind to the Hox/Exd/Hth DNA binding motifs, and the lack of *Dll* repression
434 of collembolan Ubx does not appear to be related to any deficiencies in DNA binding
435 capacity. This implies that the mechanisms underlying the absence of repression may
436 stem from other aspects of the regulation progress.

437

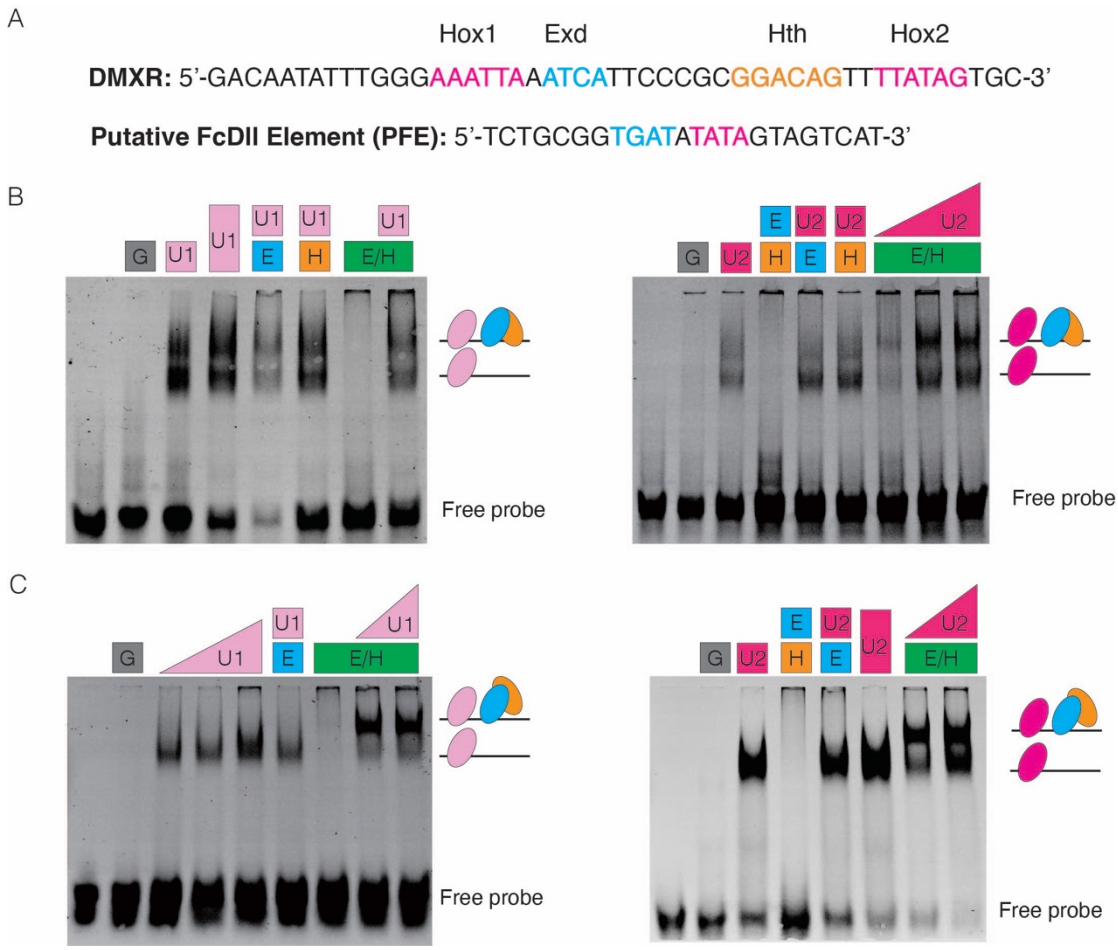

Figure 4 Collembolan Ubx and its cofactors could bind to the DNA elements that contain Hox/Exd/Hth binding motifs.

A. DNA probes used for EMSAs. DMXR, the transcription regulatory element of *D. melanogaster Dll* (Gebelein et al., 2002; Gebelein et al., 2004); Putative FcDll Element (PFE), a screened DNA region of *F. candida*, containing the Hox and Exd binding motifs. The binding sites of Hox/Exd/Hth are shown in colours. **B, C.** Assemblies of collembolan Ubx/Exd/Hth on DMXR and Putative FcDll Element (PFE), respectively. G, GST; U1, FcU1; U2, FcU2; E, Exd; H, Hth. Simplified complexes are indicated on the right.

449 **The C-terminus of FcUbx contains both repression and regulatory domains**

450 Next, to evaluate the transcriptional activity of Collembolan Ubx on *Dll*, we carried out
451 dual luciferase assays in *Drosophila* S2 cells. This involved assessing the repression
452 capacity of various proteins (Figure 5A, Supplementary Data 5), including the complete,
453 truncated, and chimeric forms of both collembolan and *Drosophila* Ubx proteins on the
454 expression of the firefly luciferase reporter gene under the regulation of the DMXR
455 element (Figure 4A, 5A, Supplementary Data 7).

456 Although previous research reported that collembolan Ubx cannot repress *Dll* (Palopoli
457 & Patel, 1998), surprisingly, our results revealed that the two isoforms of collembolan
458 Ubx (FcU1 and FcU2) were capable of inhibiting the expression of the firefly luciferase
459 reporter gene (Figure 5B), which could support our hypothesis that Ubx could repress
460 *Dll* expression during the stages of appendage maturation (Figure 3G). For collembolan
461 Ubx, the linker region is not required for the repression function; In contrast, the longest
462 linker is indispensable for the repression function of *Drosophila* Ubx, as the non-linker
463 isoform of *Drosophila* Ubx (DmUbx_IVa) and the chimeric protein Dm/Fc_L (Linker
464 of *Drosophila* Ubx is replaced by a short linker GQSYL from *F. candida*) significantly
465 lost its repression capability (Figure 5B).

466 Gebelein et al. revealed that the truncated form of the *Drosophila* Ubx C-terminus is
467 partially able to repress *Dll* (Gebelein et al., 2002). In contrast, our repression assay
468 showed that the truncation of FcU1 and FcU2, which lack a C-terminus (FcU1△C and
469 FcU2△C), significantly decreased their repression ability (Figure 5B), indicating that
470 the C-terminus may contain a potential transcriptional inhibitory domain. Unexpectedly,
471 the chimeric protein Dm/Fc_C (C-terminus of *Drosophila* Ubx is replaced by a short
472 C-terminus AKADCKSVY from *F. candida*) exhibited a substantial loss of repression
473 capacity when compared to DmUbx_Ib, suggesting that the C-terminus of collembolan
474 Ubx (AKADCKSVY) probably contains potential regulatory or modification site(s)
475 that are capable of regulating the repression function of DmUbx_Ib (Figure 5, 6B).

476 Collectively, our results indicate that the linker of FcUbx is unnecessary for the

477 repression function, while the C-terminus may exhibit both a repression domain
478 (QAQA domain) and a functional regulatory site (S) (Figure 6). These findings provide
479 functional evidence on the mechanisms of Ubx-mediated gene repression.

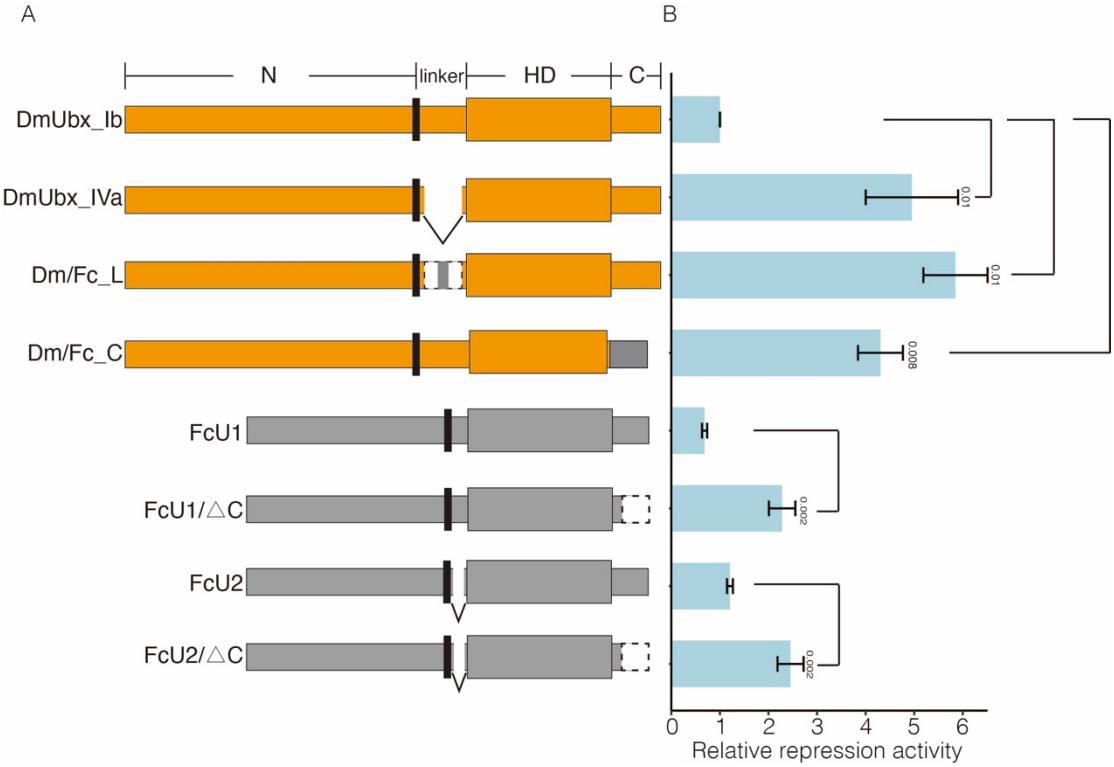

480

481 **Figure 5 Collembolan Ubx could repress *Dll* transcription while its C-terminus**
482 **contains regulatory domain(s).**

483 **A.** Constructs of proteins used for transcription repression assays, including complete
484 sequences, chimaeras, and truncations of *D. melanogaster* (yellow shade) and *F.*
485 *candida* (grey shade) Ubx. Dm/Fc_L, the linker of DmUbx_Ib was replaced by the
486 linker (GQSYL) of FcU; Dm/Fc_C, the C-terminus of DmUbx_Ib was replaced by the
487 C-terminus (AKADCKSVY) of FcU; FcU1△C and FcU2△C, the C-terminus (QAQA
488 AKADCKSVY) of FcUbx were deleted. **B.** The relative transcriptional repressive
489 activity of Ubx. The number on the Y-axis indicates transcriptional repression activity
490 relative to DmUbx_Ib. Significant P values of selected pairwise comparisons are shown
491 (Student's t-test).
492

493 **The sequence evolution of linker and C-terminus in arthropod Ubx**

494 The regulatory functions of the linker and C-terminus of Ubx in *D. melanogaster* and
495 *F. candida* suggest their significant roles in the evolution and regulation of arthropod
496 abdominal appendage formation. To depict the evolutionary trajectory of those
497 sequence features, we compared Ubx sequences from diverse representatives of
498 panarthropods, including Insecta, Diplura, Collembola, Protura, Crustacea, Myriapoda,
499 Chelicerate, and Onychophoran (Supplementary Data 4).

500 As illustrated in the multiple sequence alignment of Ubx across panarthropods (Figure
501 6), *D. melanogaster* (DmUbx_Ib) exhibits the longest linker region, consisting of more
502 than 40 amino acids. Nevertheless, the Ubx from proturan (SeUbx), and collembolans
503 (FcUbx1, OcUbx) display markedly shorter linker regions, typically composed of only
504 3-5 amino acids. In certain species, this linker region may be absent. Remarkably, the
505 sequences of the C-terminus display evolutionary patterns. In Crustaceans, their Ubx
506 (AfUbx, DmUbx) consistently maintain potential Ser/Thr (S/T) phosphorylation sites
507 (Ronshaugen et al., 2002) (Figure 6). In contrast, the insects, characterized by the loss
508 of abdominal appendages in adult stages, feature a QAQA domain and poly-Ala
509 stretches instead of phosphorylation sites (Galant & Carroll, 2002; Ronshaugen et al.,
510 2002) in their Ubx (DmUbx_Ib, DmUbx_IVa, DdUbx, MdUbx, AmUbx and TcUbx)
511 (Figure 6). Interestingly, in the three groups of basal hexapods, proturans maintain short,
512 cylindrical appendages on the first three abdominal segments (Headrick & Gordh,
513 2009), diplurans possess a pair of cerci at the last abdominal segments (Headrick &
514 Gordh, 2009), and their Ubx (proturan SeUbx and dipluran CaUbx) have QAQA
515 domains, poly-Ala stretches and S/T sites. Meanwhile, in Collembola, which bears
516 three types of abdominal appendages (Figure 1C), the collembolans Ubx (FcUbx and
517 OcUbx) lack poly-Ala stretches but contain the QAQA domains and a putative
518 phosphorylated site Ser (S) in FcUbx (Figure 6).

519 Genes with similar expression patterns usually participate in the same biological
520 process (Ala et al., 2008; Bar-Joseph, 2004; Bhar et al., 2013; van Dam et al., 2018).

521 To infer the potential regulation of collembolan Ubx, we conducted Spearman
522 correlation ($r > 0.95$, $p < 0.01$) analysis throughout embryogenesis (E_0.5d to E_9.5d)
523 and identified a total of 113 genes with 287 transcripts coexpressed with *Ubx*, including
524 the Hox gene *AbdA*. We also found phosphorylation kinase receptors (*ROR*) and
525 phosphatases (*Ptp69D*, *Ptp99A*) (Supplementary Data 8). Given the sequence
526 comparison and functions of FcUbx, we hypothesize that collembolan Ubx may
527 undergo direct or indirect regulation by protein phosphorylation and dephosphorylation
528 during embryogenesis.
529

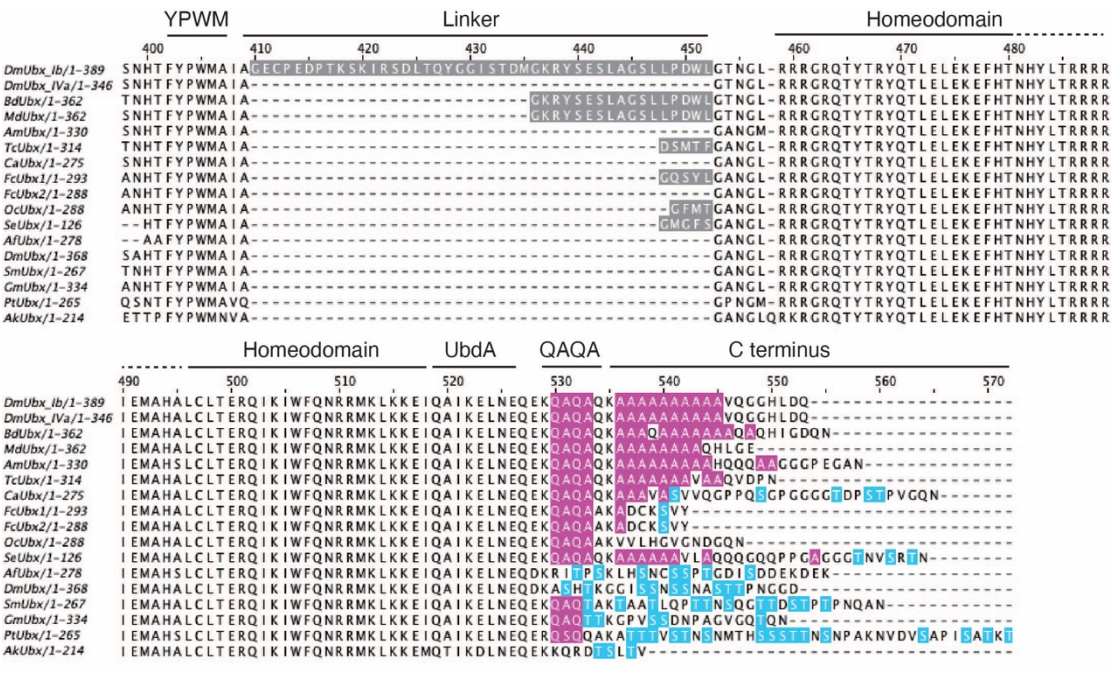

Figure 6 Sequence comparison of the linker and C-terminus of the panarthropod Ubx

Partial multiple sequence alignment of Ubx across Panarthropoda, encompassing Insecta, Diplura, Collembola, Protura, Crustacea, Myriapoda, Chelicerata and Onychophora. Insecta: *Drosophila melanogaster* (DmUbx_Ib, DmUbx_IVa), *Bactrocera dorsalis* (BdUbx), *Musca domestica* (MdUbx), *Apis mellifera* (AmUbx), *Tribolium castaneum* (TcUbx); Diplura: *Campodea augens* (CaUbx); Collembola: *Folsomia candida* (FcUbx1, FcUbx2), *Orchesella cincta* (OcUbx); Protura: *Sinentomon erythranum* (SeUbx); Crustacea: *Artemia franciscana* (AfUbx), *Daphnia magna* (DmUbx); Myriapoda: *Strigamia maritima* (SmUbx), *Glomeris marginata* (GmUbx); Chelicerata: *Parasteatoda tepidariorum* (PtUbx); Onychophora: *Acanthokara kaputensis* (AkUbx). The functional domains are indicated. YPWM, YPWM motif; UbdA, UbdA motif. Features of sequences are highlighted in colours. The QAQA domain and poly-Ala stretch are marked in pink, and putative phosphorylated sites S/T (Ser/Thr) are marked in blue. Linkers are marked in grey.

547 **Discussion**

548 **Genes involved in the development of collembolan appendages**

549 Collembola, as a basal hexapod group, exhibits morphological traits that intermediate
550 between crustaceans and insects (Gao et al., 2008; Luan et al., 2005; Misof et al., 2014).
551 Exploring the evolutionary and developmental mechanisms underlying these
552 phenotypes could provide valuable insights into the terrestrialization of hexapods (van
553 Straalen, 2021). In this study, we employed two distinct data mining approaches to
554 comprehensively identify genes involved in collembolan appendage development.

555 The first approach, the "transcriptome-wide screening strategy," involves selecting
556 specific appendage formation stages to identify genes that follow the predefined
557 developmental trajectory. We identified several relevant appendage formation genes,
558 such as *Notch*, *En*, *Scr*, *Antp*, *Ubx*, *Exd*, *Hth* and *Lim1* (Table 1), which have been
559 extensively studied in *D. melanogaster* for decades. Engrailed controls the
560 segmentation of embryo (van de Heuvel et al., 1993) and Notch regulates the
561 segmentation of leg (de Celis et al., 1998; Rauskolb & Irvine, 1999); Hox genes Scr,
562 Antp, Ubx are required for the thoracic segment identity (Kaufman & Abbott, 1984),
563 Antp controls the formation of leg (Struhl, 1982) and Ubx repress the abdomen leg
564 (Castelli-Gair & Akam, 1995; Gebelein et al., 2002). Exd, Hth and Lim1 are essential
565 for establishing the proximal-distal axis of limbs and regulating the formation of the
566 coxa, femur, tibia and tarsus (Costello et al., 2015; Ruiz-Losada et al., 2018; Tsuji et al.,
567 2000).

568 The second approach, the "candidate-gene focusing strategy", is designed by focusing
569 on the pivotal *Ubx* gene and extracting coexpressed genes during embryogenesis. This
570 analysis not only uncovered the canonical *AbdA* genes (Averof & Patel, 1997; Casares
571 et al., 1996; Konopova & Akam, 2014) but also identified genes related to appendage
572 formation (Supplementary Data 8), including *Lim1* and *DAAM.* In *D. melanogaster*, the
573 deletion of DAAM results in abnormalities in actin filament structures (Barkó et al.,
574 2010; Prokop et al., 2011).

575 These two synergistic approaches have elucidated a set of genes that have not
576 undergone extensive investigation in arthropods except for *D. melanogaster*. Our
577 analysis introduces new perspectives and broadens the scope of research directions.
578 However, it is crucial to note that the transcriptomes we examined were derived from
579 whole animals, and the identified genes might also be involved in various biological
580 processes, such as organogenesis and neurogenesis. Further research studies are
581 necessary to verify the functional roles of these genes during collembolan appendage
582 development.
583
584 **The evolution of functional domains in arthropod Ubx**
585 Throughout its evolution, arthropod Ubx progressively acquired the capacity to inhibit
586 *Dll* expression in the abdomen of insect adults, consequently resulting in the loss of
587 abdominal appendages (Jockusch & Smith, 2015). In this study, by integrating
588 functional assays in collembolan Ubx, we reconstructed the evolutionary trajectory of
589 functional domains in Ubx (Figure 7, Table 2): (1) The ancestral Ubx in Panarthropoda
590 (onychophorans and arthropods) exhibited a consistent DNA binding capability (Galant
591 & Carroll, 2002; Gebelein et al., 2004; Ronshaugen et al., 2002). However, their
592 effectiveness in inhibiting the downstream target *Dll* varied among species (Table 2)
593 (Galant & Carroll, 2002; Gebelein et al., 2002; Grenier & Carroll, 2000; Ronshaugen
594 et al., 2002). (2) In Crustacea, the crustacean Ubx (AfUbx) is unable to inhibit *Dll*, and
595 previous research has proposed that potential regulatory phosphorylation sites may be
596 located in the C-terminus of AfUbx (Galant & Carroll, 2002; Ronshaugen et al., 2002).
597 (3) In Hexapoda, *Drosophila* Ubx (DmUbx_Ib) robustly represses *Dll* expression, the
598 linker region and the C-terminus (including both the QAQA domain and the poly-Ala
599 stretch) play crucial roles in this regulatory process (Galant & Carroll, 2002; Gebelein
600 et al., 2002; Ronshaugen et al., 2002). (4) Remarkably, collembolan Ubx demonstrated
601 the ability to inhibit *Drosophila Dll* expression, mirroring the capability observed in
602 DmUbx_Ib (Figure 5). Nonetheless, (5) unlike *Drosophila* Ubx, the linker region of

603 collembolan Ubx was not essential for this repression (Figure 6). Rather, (6) it appeared
604 that the functional repression domain and potential regulatory phosphorylation sites
605 may be in the C-terminus of collembolan Ubx (Figure 5, 6).
606 On the basis of these results, we summarize and propose a functional mechanism of
607 how the collembolan Ubx suppresses *Dll* transcription that appears to be intermediate
608 between that of crustaceans and insects (Table 2). Moreover, given the evidence of
609 characters (QAQA domain, poly Ala stretch and S/T site) in the C-terminus of dipluran
610 and proturan Ubx (Figure 6), we speculate that the ancestral hexapod Ubx could bind
611 and repress the expression of *Dll*. However, the scarcity of Ubx sequences in basal
612 hexapods limits our understanding. Currently, only two complete collembolan Ubx
613 sequences are publicly available (FcUbx and OcUbx), exhibiting inconsistencies in
614 sequence features (Figure 6). With the advancement of genomic sequencing techniques,
615 we anticipate that more Ubx sequences could be extracted from the genomes of basal
616 hexapods. This, in turn, would facilitate the consolidation of sequence features in
617 hexapods and enlighten the exploration of the evolutionary trajectory of functional
618 domains in arthropod Ubx.

619

620 **Table 2** Functional evolution of Ubx.

	DNA binding	**Functional dissection of Ubx on *Dll* repression**			
		Repression capacity of complete protein	Indispensability of linker	C-terminus	
				Repression domain	Phosphorylation site
AkUbx	+	-	-	ND	+
AfUbx	ND	-	-	-	+
FcUbx	+	+	-	+	+
DmUbx	+	+	+	+	-

621 **Figure 7.** Schematic summary of the functional domains in Ubx of panarthropods. **Note**: +: strong phenotype; -: no phenotype; ND: no data

622 **The regulatory mechanism of collembolan Ubx on *Dll***

623 It is essential to highlight that the discussion on the functional evolution of Ubx
624 primarily relies on the mechanism through which arthropod Ubx suppresses *Drosophila*
625 *Dll*, and the *bona fide* mechanism of how arthropod Ubx (*trans-factor*) interacts with
626 endogenous regulatory element of *Dll* (*cis-element*) remains underexplored. In
627 combination with our functional assays and transcriptomic analyses, we propose a
628 model to discuss the potential mechanism of how collembolan Ubx regulates the
629 abdominal segments: collembolan Ubx exhibits binding and repression of *Dll*
630 expression uniformly across all segments at the abdominal appendage formation stage
631 (Figures 3F, 4C, 5). Nevertheless, within each of the abdominal segments, collembolan
632 Ubx implements its repression function in a spatially and temporally context-specific
633 manner as depicted in our model (Figure 8). During the early abdominal appendage
634 formation stage (E_3.5d) in abdominal segments 1 and 3 (A1 and A3), Ubx is likely
635 subject to protein phosphorylation, potentially related to Ror (Table 1, Supplementary
636 Data 2, 8). This phosphorylation impairs repression on *Dll*, thereby promoting the
637 development of the ventral tube and retinaculum. We propose that distinct
638 morphologies of these abdominal appendages may be influenced by different cofactors,
639 potentially contributing to morphological malformations, such as Lim1 and CG7526
640 (Table 1, Supplementary Data 8). We hypothesis two scenarios for abdominal segment
641 2 (A2) or the appendage maturation stages (E_5.5d onwards): (H1) Ubx undergoes
642 dephosphorylation by phosphatases Ptp69D or Ptp99A (Supplementary Data 8),
643 allowing it to exert its repression function on *Dll*, resulting in the absence of appendages
644 in A2; or (H2) it is still possible that the chromatin landscape of the *Dll* regulatory
645 region becomes inaccessible, thus preventing *Dll* transcription and appendage
646 formation.

647 Despite the current scarcity of genetic tools in collembolans, the confirmation of our
648 model demands leveraging cutting-edge experiments and functional genomics
649 techniques. For instance, ChIP-seq (Park, 2009) or CUT& TAG (Kaya-Okur et al., 2019)

allow the identification of Ubx-*Dll* interaction in a genome-wide scale. Additionally, employing the CRISPR/CAS technology (Akinci et al., 2021) to manipulate the Putative FcDll Element would validate its role as a transcriptional regulatory element in collembolans. Furthermore, the incorporation of spatial transcriptomics (Marx, 2021) and spatial ATAC-seq (Deng et al., 2022) to comprehensively map the intricate context of transcription factors and the regulatory landscape in each segment. These methodologies will empower us to investigate how Ubx works precisely, provide compelling evidence for holistic reconstruction of its functional evolution, and ultimately shed light on how arthropods lost their abdominal appendages during evolution.

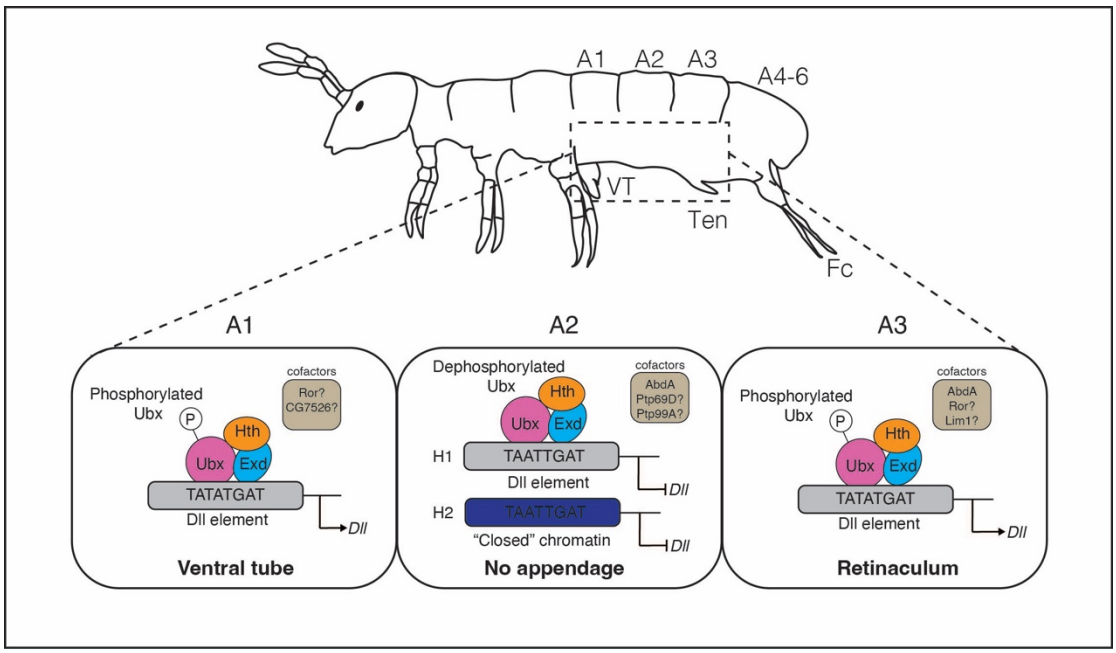

Figure 8 The proposed model for the regulation of collembolan Ubx on *Dll*

A schematic morphology of adult *F. candida*. The abdominal segments are shown as A1 to A6. VT, ventral tube; Ten, retinaculum; Fc, furca. The functional regulatory model of Ubx: in A1 and 3, Ubx is phosphorylated, resulting in the derepression of *Dll* and facilitating the formation of appendages; Conversely, in A2, (H1) Ubx exerts its repression function on *Dll* expression; or (H2) the chromatin of *Dll* regulatory region is "closed", therefore suppressing appendage formation. See the text in the discussion for a detailed explanation.

670 **Abbreviation**

671 **Ubx:** *Ultrabithorax*

672 **AbdA**: *Abdominal A*

673 **Exd**: *Extradentical*

674 **Hth**: *Homothorax*

675 **Dll**: *Distal-less*

676 **Vt:** Ventral tube

677 **Ten**: Retinaculum

678 **Fc**: Furca

679 **An**: antenna

680 **AnS**: antenna segment

681 **Cllr**: clypeolabrum

682 **DO**: dorsal organ

683 **IcS**: intercalary segment

684 **MdS**: mandibular segment

685 **SEM**: Scanning electron microscopy

686 **STEM**: Short Time-series Expression Miner

687 **RPKM**: reads per kilobase per million

688 **GO term**: Gene Ontology term

689 **KEGG pathway**: Kyoto Encyclopedia of Genes and Genomes

690 **IPTG**: isopropyl β-D-1-thiogalactopyranoside

691 **GST**: Glutathione S-transferase

692 **DMXR**: the transcription regulatory element of *D. melanogaster Dll304*

693 **PFE**: Putative FcDll Element

694 **EMSA**: Electrophoretic mobility shift assay

695

696 **Supplementary Data**

697 1. The gene expression dynamics of *F. candida*

698 2. Short Time-series Expression Miner analysis

699 3. The GO annotation and KEGG pathways of Cluster 42

700 4. Multiple sequence alignment of Ubx

701 5. Truncated proteins of Ubx/Exd/Hth

702 6. Genomic sequence of *F. candida Dll*

703 7. Dual luciferase assays of collembolan and *Drosophila* proteins

704 8. Genes coexpressed with *FcUbx*

705

706 **Authors' contributions**

707 Y.L. and Y.-X.L. conceived the project. Y.L. performed all the experiments and data
708 analyses and drafted the manuscript. The authors read and approved the manuscript.

709

710 **Funding**

711 The National Natural Science Foundation of China (32170425, 31970438)

712

713 **Acknowledgements**

714 We thank all the lab members from Yin and Luan's previous laboratory for their help
715 and valuable discussion about this work. We would like to express appreciation to many
716 colleagues. Dr. WU Wei and the team from the Core Facility of Drosophila Resource
717 and Technology at the Centre for Excellence in Molecular Cell Science, CAS for their
718 assistance in establishing the transgenic fly strains of collembolan Ubx and providing
719 troubleshooting support. Miss LI Jiqing and Mr GAO Xiaoyan from the Electron
720 Microscope Platform at the Centre for Excellence in Molecular Plant Sciences, CAS
721 for the aid in the SEM of the collembolans. Dr. ZHAO Qin and Dr. WANG Jing for
722 their suggestions on protein expression. Dr. HE Juanmei and Dr. LANG Nannan for
723 generously sharing the EMSA protocol. Dr. JIA Qiangqiang for assistance with
724 luciferase assays in *Drosophila* S2 cells. Dr. ZHANG Yu for help in bioinformatic
725 analysis. Dr. Chema Martin at Queen Mary University of London and Dr. Kamil Jaron
726 at Wellcome Sanger Institute for the comments on the manuscript.

727

References

Akinci, E., Hamilton, M. C., Khowpinitchai, B., & Sherwood, R. I. (2021). Using CRISPR to understand and manipulate gene regulation. *Development*, *148*(9). https://doi.org/10.1242/dev.182667

Ala, U., Piro, R. M., Grassi, E., Damasco, C., Silengo, L., Oti, M., Provero, P., & Di Cunto, F. (2008). Prediction of human disease genes by human-mouse conserved coexpression analysis. *PLoS Comput Biol*, *4*(3), e1000043. https://doi.org/10.1371/journal.pcbi.1000043

Altschul, S. F., Gish, W., Miller, W., Myers, E. W., & Lipman, D. J. (1990). Basic local alignment search tool. *J Mol Biol*, *215*(3), 403-410. https://doi.org/10.1016/s0022-2836(05)80360-2

Angelini, & Kaufman. (2005a). Comparative Developmental Genetics and the Evolution of Arthropod Body Plans. *Annual Review of Genetics*, *39*(1), 95-119. https://doi.org/10.1146/annurev.genet.39.073003.112310

Angelini, & Kaufman. (2005b). Insect appendages and comparative ontogenetics. *Dev Biol*, *286*(1), 57-77. https://doi.org/10.1016/j.ydbio.2005.07.006

Averof, M., & Patel, N. H. (1997). Crustacean appendage evolution associated with changes in Hox gene expression. *Nature*, *388*(6643), 682-686. https://doi.org/10.1038/41786

Bairoch, A., Apweiler, R., Wu, C. H., Barker, W. C., Boeckmann, B., Ferro, S., Gasteiger, E., Huang, H., Lopez, R., Magrane, M., Martin, M. J., Natale, D. A., O'Donovan, C., Redaschi, N., & Yeh, L. S. (2005). The Universal Protein Resource (UniProt). *Nucleic Acids Res*, *33*(Database issue), D154-159. https://doi.org/10.1093/nar/gki070

Bar-Joseph, Z. (2004). Analyzing time series gene expression data. *Bioinformatics*, *20*(16), 2493-2503. https://doi.org/10.1093/bioinformatics/bth283

Bar-Joseph, Z., Gitter, A., & Simon, I. (2012). Studying and modelling dynamic biological processes using time-series gene expression data. *Nature Reviews Genetics*, *13*(8), 552-564. https://doi.org/10.1038/nrg3244

Barkó, S., Bugyi, B., Carlier, M. F., Gombos, R., Matusek, T., Mihály, J., & Nyitrai, M. (2010). Characterization of the biochemical properties and biological function of the formin homology domains of Drosophila DAAM. *J Biol Chem*, *285*(17), 13154-13169. https://doi.org/10.1074/jbc.M109.093914

Berger, M. F., Badis, G., Gehrke, A. R., Talukder, S., Philippakis, A. A., Peña-Castillo, L., Alleyne, T. M., Mnaimneh, S., Botvinnik, O. B., Chan, E. T., Khalid, F., Zhang, W., Newburger, D., Jaeger, S. A., Morris, Q. D., Bulyk, M. L., & Hughes, T. R. (2008). Variation in homeodomain DNA binding revealed by high-resolution analysis of sequence preferences. *Cell*, *133*(7), 1266-1276. https://doi.org/10.1016/j.cell.2008.05.024

Bhar, A., Haubrock, M., Mukhopadhyay, A., Maulik, U., Bandyopadhyay, S., & Wingender, E. (2013). Coexpression and coregulation analysis of time-series gene expression data in estrogen-induced breast cancer cell. *Algorithms Mol*

Biol, *8*(1), 9. https://doi.org/10.1186/1748-7188-8-9

Brower, D. L. (1986). Engrailed gene expression in Drosophila imaginal discs. *Embo j*, *5*(10), 2649-2656. https://doi.org/10.1002/j.1460-2075.1986.tb04547.x

Brown, J. B., Boley, N., Eisman, R., May, G. E., Stoiber, M. H., Duff, M. O., Booth, B. W., Wen, J., Park, S., Suzuki, A. M., Wan, K. H., Yu, C., Zhang, D., Carlson, J. W., Cherbas, L., Eads, B. D., Miller, D., Mockaitis, K., Roberts, J., Davis, C. A., Frise, E., Hammonds, A. S., Olson, S., Shenker, S., Sturgill, D., Samsonova, A. A., Weiszmann, R., Robinson, G., Hernandez, J., Andrews, J., Bickel, P. J., Carninci, P., Cherbas, P., Gingeras, T. R., Hoskins, R. A., Kaufman, T. C., Lai, E. C., Oliver, B., Perrimon, N., Graveley, B. R., & Celniker, S. E. (2014). Diversity and dynamics of the Drosophila transcriptome. *Nature*, *512*(7515), 393-399. https://doi.org/10.1038/nature12962

Browne, W. E., & Patel, N. H. (2000). Molecular genetics of crustacean feeding appendage development and diversification. *Seminars in Cell & Developmental Biology*, *11*(6), 427-435. https://doi.org/https://doi.org/10.1006/scdb.2000.0196

Budd, G. E., & Telford, M. J. (2009). The origin and evolution of arthropods. *Nature*, *457*(7231), 812-817. https://doi.org/10.1038/nature07890

Buffry, A. D., Kittelmann, S., & McGregor, A. P. (2023). Characterisation of the role and regulation of Ultrabithorax in sculpting fine-scale leg morphology [Original Research]. *Frontiers in Cell and Developmental Biology*, *11*. https://doi.org/10.3389/fcell.2023.1119221

Casares, F., Calleja, M., & Sánchez-Herrero, E. (1996). Functional similarity in appendage specification by the Ultrabithorax and abdominal-A Drosophila HOX genes. *Embo j*, *15*(15), 3934-3942. https://www.ncbi.nlm.nih.gov/pmc/articles/PMC452108/pdf/emboj00015-0170.pdf

Castelli-Gair, J., & Akam, M. (1995). How the Hox gene Ultrabithorax specifies two different segments: the significance of spatial and temporal regulation within metameres. *Development*, *121*(9), 2973-2982. https://doi.org/10.1242/dev.121.9.2973

Cohen, B., Simcox, A. A., & Cohen, S. M. (1993). Allocation of the thoracic imaginal primordia in the Drosophila embryo. *Development*, *117*(2), 597-608. https://doi.org/10.1242/dev.117.2.597

Cohen, B., Wimmer, E. A., & Cohen, S. M. (1991). Early development of leg and wing primordia in the Drosophila embryo. *Mech Dev*, *33*(3), 229-240. https://doi.org/10.1016/0925-4773(91)90030-a

Cohen, S. M. (1990). Specification of limb development in the Drosophila embryo by positional cues from segmentation genes. *Nature*, *343*(6254), 173-177. https://doi.org/10.1038/343173a0

Conesa, A., Götz, S., García-Gómez, J. M., Terol, J., Talón, M., & Robles, M. (2005). Blast2GO: a universal tool for annotation, visualization and analysis in functional genomics research. *Bioinformatics*, *21*(18), 3674-3676.

https://doi.org/10.1093/bioinformatics/bti610

Costello, I., Nowotschin, S., Sun, X., Mould, A. W., Hadjantonakis, A. K., Bikoff, E. K., & Robertson, E. J. (2015). Lhx1 functions together with Otx2, Foxa2, and Ldb1 to govern anterior mesendoderm, node, and midline development. *Genes Dev*, *29*(20), 2108-2122. https://doi.org/10.1101/gad.268979.115

de Celis, J. F., Tyler, D. M., de Celis, J., & Bray, S. J. (1998). Notch signalling mediates segmentation of the Drosophila leg. *Development*, *125*(23), 4617-4626. https://doi.org/10.1242/dev.125.23.4617

Deng, Y., Bartosovic, M., Ma, S., Zhang, D., Kukanja, P., Xiao, Y., Su, G., Liu, Y., Qin, X., Rosoklija, G. B., Dwork, A. J., Mann, J. J., Xu, M. L., Halene, S., Craft, J. E., Leong, K. W., Boldrini, M., Castelo-Branco, G., & Fan, R. (2022). Spatial profiling of chromatin accessibility in mouse and human tissues. *Nature*, *609*(7926), 375-383. https://doi.org/10.1038/s41586-022-05094-1

Durston, A. J., Jansen, H. J., In der Rieden, P., & Hooiveld, M. H. (2011). Hox collinearity - a new perspective. *Int J Dev Biol*, *55*(10-12), 899-908. https://doi.org/10.1387/ijdb.113358ad

Ekker, S. C., Young, K. E., von Kessler, D. P., & Beachy, P. A. (1991). Optimal DNA sequence recognition by the Ultrabithorax homeodomain of Drosophila. *Embo j*, *10*(5), 1179-1186. https://doi.org/10.1002/j.1460-2075.1991.tb08058.x

Ernst, J., & Bar-Joseph, Z. (2006). STEM: a tool for the analysis of short time series gene expression data. *BMC Bioinformatics*, *7*, 191. https://doi.org/10.1186/1471-2105-7-191

Ernst, J., Nau, G. J., & Bar-Joseph, Z. (2005). Clustering short time series gene expression data. *Bioinformatics*, *21 Suppl 1*, i159-168. https://doi.org/10.1093/bioinformatics/bti1022

Faddeeva-Vakhrusheva, A., Kraaijeveld, K., Derks, M. F. L., Anvar, S. Y., Agamennone, V., Suring, W., Kampfraath, A. A., Ellers, J., Le Ngoc, G., van Gestel, C. A. M., Mariën, J., Smit, S., van Straalen, N. M., & Roelofs, D. (2017). Coping with living in the soil: the genome of the parthenogenetic springtail Folsomia candida. *BMC Genomics*, *18*(1), 493. https://doi.org/10.1186/s12864-017-3852-x

Fountain, M. T., & Hopkin, S. P. (2005). Folsomia candida (Collembola): a "standard" soil arthropod. *Annu Rev Entomol*, *50*(Volume 50, 2005), 201-222. https://doi.org/10.1146/annurev.ento.50.071803.130331

Fountain, M. T., & Hopkin, S. P. (2005). FOLSOMIA CANDIDA (COLLEMBOLA): A “Standard” Soil Arthropod. *Annual Review of Entomology*, *50*(1), 201-222. https://doi.org/10.1146/annurev.ento.50.071803.130331

Galant, R., & Carroll, S. B. (2002). Evolution of a transcriptional repression domain in an insect Hox protein. *Nature*, *415*(6874), 910-913. https://doi.org/10.1038/nature717

Gao, Y., Bu, Y., Luan, Y.-X., & Yin, W.-Y. (2006). Preliminary Observation on the Embryonic Development of Folsomia candida (Collembola: Isotomidae). *Zoological Research*, *5*(27), 519-524.

Gao, Y., Bu, Y., & Luan, Y. X. (2008). Phylogenetic relationships of basal hexapods reconstructed from nearly complete 18S and 28S rRNA gene sequences. *Zoolog Sci*, *25*(11), 1139-1145. https://doi.org/10.2108/zsj.25.1139

Gaunt, S. J. (2015). The significance of Hox gene collinearity. *Int J Dev Biol*, *59*(4-6), 159-170. https://doi.org/10.1387/ijdb.150223sg

Gebelein, B., Culi, J., Ryoo, H. D., Zhang, W., & Mann, R. S. (2002). Specificity of Distalless repression and limb primordia development by abdominal Hox proteins. *Dev Cell*, *3*(4), 487-498. https://doi.org/10.1016/s1534-5807(02)00257-5

Gebelein, B., McKay, D. J., & Mann, R. S. (2004). Direct integration of Hox and segmentation gene inputs during Drosophila development. *Nature*, *431*(7009), 653-659. https://doi.org/10.1038/nature02946

Geyer, A., Koltsaki, I., Hessinger, C., Renner, S., & Rogulja-Ortmann, A. (2015). Impact of Ultrabithorax alternative splicing on Drosophila embryonic nervous system development. *Mechanisms of Development*, *138*, 177-189. https://doi.org/https://doi.org/10.1016/j.mod.2015.08.007

Giribet, G., Edgecombe, G. D., & Wheeler, W. C. (2001). Arthropod phylogeny based on eight molecular loci and morphology. *Nature*, *413*(6852), 157-161. https://doi.org/10.1038/35093097

Grenier, J. K., & Carroll, S. B. (2000). Functional evolution of the Ultrabithorax protein. *Proc Natl Acad Sci U S A*, *97*(2), 704-709. https://doi.org/10.1073/pnas.97.2.704

He, J. M., Zhu, H., Zheng, G. S., Liu, P. P., Wang, J., Zhao, G. P., Zhu, G. Q., Jiang, W. H., & Lu, Y. H. (2016). Direct Involvement of the Master Nitrogen Metabolism Regulator GlnR in Antibiotic Biosynthesis in Streptomyces. *J Biol Chem*, *291*(51), 26443-26454. https://doi.org/10.1074/jbc.M116.762476

Headrick, D. H., & Gordh, G. (2009). Chapter 5 - Anatomy: Head, Thorax, Abdomen, and Genitalia. In V. H. Resh & R. T. Cardé (Eds.), *Encyclopedia of Insects (Second Edition)* (pp. 11-21). Academic Press. https://doi.org/https://doi.org/10.1016/B978-0-12-374144-8.00005-9

Hughes, & Kaufman. (2002a). Exploring the myriapod body plan: expression patterns of the ten Hox genes in a centipede. *Development*, *129*(5), 1225-1238. https://doi.org/10.1242/dev.129.5.1225

Hughes, & Kaufman. (2002b). Hox genes and the evolution of the arthropod body plan. *Evol Dev*, *4*(6), 459-499. https://doi.org/10.1046/j.1525-142x.2002.02034.x

Jockusch, E. L., & Smith, F. W. (2015). Hexapoda: Comparative Aspects of Later Embryogenesis and Metamorphosis. In A. Wanninger (Ed.), *Evolutionary Developmental Biology of Invertebrates 5: Ecdysozoa III: Hexapoda* (pp. 111-208). Springer Vienna. https://doi.org/10.1007/978-3-7091-1868-9_3

Jockusch, E. L., Williams, T. A., & Nagy, L. M. (2004). The evolution of patterning of serially homologous appendages in insects. *Development Genes and Evolution*, *214*(7), 324-338. https://doi.org/10.1007/s00427-004-0412-6

Kanehisa, M., & Goto, S. (2000). KEGG: kyoto encyclopedia of genes and genomes. *Nucleic Acids Res*, *28*(1), 27-30. https://doi.org/10.1093/nar/28.1.27

Kaufman, T. C., & Abbott, M. K. (1984). Homoeotic Genes and the Specification of Segmental Identity in the Embryo and Adult Thorax of Drosophila Melanogaster. In G. M. Malacinski & W. H. Klein (Eds.), *Molecular Aspects of Early Development* (pp. 189-218). Springer US. https://doi.org/10.1007/978-1-4684-4628-9_9

Kaya-Okur, H. S., Wu, S. J., Codomo, C. A., Pledger, E. S., Bryson, T. D., Henikoff, J. G., Ahmad, K., & Henikoff, S. (2019). CUT&Tag for efficient epigenomic profiling of small samples and single cells. *Nature Communications*, *10*(1), 1930. https://doi.org/10.1038/s41467-019-09982-5

Kim, D., Pertea, G., Trapnell, C., Pimentel, H., Kelley, R., & Salzberg, S. L. (2013). TopHat2: accurate alignment of transcriptomes in the presence of insertions, deletions and gene fusions. *Genome Biol*, *14*(4), R36. https://doi.org/10.1186/gb-2013-14-4-r36

Kolde, R. (2012). Pheatmap: pretty heatmaps. *R package version*, *1*(2), 726.

Konopova, B., & Akam, M. (2014). The Hox genes Ultrabithorax and abdominal-A specify three different types of abdominal appendage in the springtail Orchesella cincta (Collembola). *Evodevo*, *5*(1), 2. https://doi.org/10.1186/2041-9139-5-2

Krogh, P. H. (2009). Toxicity testing with the collembolans Folsomia fimetaria and Folsomia candida and the results of a ringtest.

Kurata, S., Go, M. J., Artavanis-Tsakonas, S., & Gehring, W. J. (2000). Notch signaling and the determination of appendage identity. *Proc Natl Acad Sci U S A*, *97*(5), 2117-2122. https://doi.org/10.1073/pnas.040556497

Langmead, B., & Salzberg, S. L. (2012). Fast gapped-read alignment with Bowtie 2. *Nat Methods*, *9*(4), 357-359. https://doi.org/10.1038/nmeth.1923

Liang, Y., Xie, W., & Luan, Y. X. (2019). Developmental expression and evolution of hexamerin and haemocyanin from Folsomia candida (Collembola). *Insect Molecular Biology*, *28*(5), 716-727. https://doi.org/https://doi.org/10.1111/imb.12585

Luan, Y. X., Cui, Y., Chen, W. J., Jin, J. F., Liu, A. M., Huang, C. W., Potapov, M., Bu, Y., Zhan, S., Zhang, F., & Li, S. (2023). High-quality genomes reveal significant genetic divergence and cryptic speciation in the model organism Folsomia candida (collembola). *Mol Ecol Resour*, *23*(1), 273-293. https://doi.org/10.1111/1755-0998.13699

Luan, Y. X., Mallatt, J. M., Xie, R. D., Yang, Y. M., & Yin, W. Y. (2005). The phylogenetic positions of three Basal-hexapod groups (protura, diplura, and collembola) based on ribosomal RNA gene sequences. *Mol Biol Evol*, *22*(7), 1579-1592. https://doi.org/10.1093/molbev/msi148

Marx, V. (2021). Method of the Year: spatially resolved transcriptomics. *Nature Methods*, *18*(1), 9-14. https://doi.org/10.1038/s41592-020-01033-y

Matsuda, R. (2017). *Morphology and evolution of the insect abdomen: with special reference to developmental patterns and their bearings upon systematics*. Elsevier.

McGinnis, S., & Madden, T. L. (2004). BLAST: at the core of a powerful and diverse set of sequence analysis tools. *Nucleic Acids Res*, *32*(Web Server issue), W20-25. https://doi.org/10.1093/nar/gkh435

McIntosh, B. B., & Ostap, E. M. (2016). Myosin-I molecular motors at a glance. *J Cell Sci*, *129*(14), 2689-2695. https://doi.org/10.1242/jcs.186403

Mead, T. J., Martin, D. R., Wang, L. W., Cain, S. A., Gulec, C., Cahill, E., Mauch, J., Reinhardt, D., Lo, C., Baldock, C., & Apte, S. S. (2022). Proteolysis of fibrillin-2 microfibrils is essential for normal skeletal development. *eLife*, *11*, e71142. https://doi.org/10.7554/eLife.71142

Misof, B., Liu, S., Meusemann, K., Peters, R. S., Donath, A., Mayer, C., Frandsen, P. B., Ware, J., Flouri, T., Beutel, R. G., Niehuis, O., Petersen, M., Izquierdo-Carrasco, F., Wappler, T., Rust, J., Aberer, A. J., Aspöck, U., Aspöck, H., Bartel, D., Blanke, A., Berger, S., Böhm, A., Buckley, T. R., Calcott, B., Chen, J., Friedrich, F., Fukui, M., Fujita, M., Greve, C., Grobe, P., Gu, S., Huang, Y., Jermiin, L. S., Kawahara, A. Y., Krogmann, L., Kubiak, M., Lanfear, R., Letsch, H., Li, Y., Li, Z., Li, J., Lu, H., Machida, R., Mashimo, Y., Kapli, P., McKenna, D. D., Meng, G., Nakagaki, Y., Navarrete-Heredia, J. L., Ott, M., Ou, Y., Pass, G., Podsiadlowski, L., Pohl, H., von Reumont, B. M., Schütte, K., Sekiya, K., Shimizu, S., Slipinski, A., Stamatakis, A., Song, W., Su, X., Szucsich, N. U., Tan, M., Tan, X., Tang, M., Tang, J., Timelthaler, G., Tomizuka, S., Trautwein, M., Tong, X., Uchifune, T., Walzl, M. G., Wiegmann, B. M., Wilbrandt, J., Wipfler, B., Wong, T. K., Wu, Q., Wu, G., Xie, Y., Yang, S., Yang, Q., Yeates, D. K., Yoshizawa, K., Zhang, Q., Zhang, R., Zhang, W., Zhang, Y., Zhao, J., Zhou, C., Zhou, L., Ziesmann, T., Zou, S., Li, Y., Xu, X., Zhang, Y., Yang, H., Wang, J., Wang, J., Kjer, K. M., & Zhou, X. (2014). Phylogenomics resolves the timing and pattern of insect evolution. *Science*, *346*(6210), 763-767. https://doi.org/10.1126/science.1257570

Monteiro, A. S., & Ferrier, D. E. K. (2006). Hox genes are not always Colinear [Review]. *International Journal of Biological Sciences*, *2*(3), 95-103. https://doi.org/10.7150/ijbs.2.95

Natori, K., Tajiri, R., Furukawa, S., & Kojima, T. (2012). Progressive tarsal patterning in the Drosophila by temporally dynamic regulation of transcription factor genes. *Developmental Biology*, *361*(2), 450-462. https://doi.org/https://doi.org/10.1016/j.ydbio.2011.10.031

Noyes, M. B., Christensen, R. G., Wakabayashi, A., Stormo, G. D., Brodsky, M. H., & Wolfe, S. A. (2008). Analysis of homeodomain specificities allows the family-wide prediction of preferred recognition sites. *Cell*, *133*(7), 1277-1289. https://doi.org/10.1016/j.cell.2008.05.023

O'Day, K. E. (2006). *Notch Signaling and Segmentation in Parhyale Hawaiensis*.

University of California, Berkeley. https://books.google.co.uk/books?id=FbFPAQAAMAAJ

Palopoli, M. F., & Patel, N. H. (1998). Evolution of the interaction between Hox genes and a downstream target. *Curr Biol*, *8*(10), 587-590. https://doi.org/10.1016/s0960-9822(98)70228-3

Panganiban, G., Irvine, S. M., Lowe, C., Roehl, H., Corley, L. S., Sherbon, B., Grenier, J. K., Fallon, J. F., Kimble, J., Walker, M., Wray, G. A., Swalla, B. J., Martindale, M. Q., & Carroll, S. B. (1997). The origin and evolution of animal appendages. *Proc Natl Acad Sci U S A*, *94*(10), 5162-5166. https://doi.org/10.1073/pnas.94.10.5162

Park, P. J. (2009). ChIP–seq: advantages and challenges of a maturing technology. *Nature Reviews Genetics*, *10*(10), 669-680. https://doi.org/10.1038/nrg2641

Passner, J. M., Ryoo, H. D., Shen, L., Mann, R. S., & Aggarwal, A. K. (1999). Structure of a DNA-bound Ultrabithorax-Extradenticle homeodomain complex. *Nature*, *397*(6721), 714-719. https://doi.org/10.1038/17833

Peel, A. D., Chipman, A. D., & Akam, M. (2005). Arthropod Segmentation: beyond the Drosophila paradigm. *Nature Reviews Genetics*, *6*(12), 905-916. https://doi.org/10.1038/nrg1724

Prokop, A., Sánchez-Soriano, N., Gonçalves-Pimentel, C., Molnár, I., Kalmár, T., & Mihály, J. (2011). DAAM family members leading a novel path into formin research. *Commun Integr Biol*, *4*(5), 538-542. https://doi.org/10.4161/cib.4.5.16511

Rauskolb, C., & Irvine, K. D. (1999). Notch-Mediated Segmentation and Growth Control of the Drosophila Leg. *Developmental Biology*, *210*(2), 339-350. https://doi.org/https://doi.org/10.1006/dbio.1999.9273

Reed, H. C., Hoare, T., Thomsen, S., Weaver, T. A., White, R. A., Akam, M., & Alonso, C. R. (2010). Alternative splicing modulates Ubx protein function in Drosophila melanogaster. *Genetics*, *184*(3), 745-758. https://doi.org/10.1534/genetics.109.112086

Ronshaugen, M., McGinnis, N., & McGinnis, W. (2002). Hox protein mutation and macroevolution of the insect body plan. *Nature*, *415*(6874), 914-917. https://doi.org/10.1038/nature716

Rozewicki, J., Li, S., Amada, K. M., Standley, D. M., & Katoh, K. (2019). MAFFT-DASH: integrated protein sequence and structural alignment. *Nucleic Acids Research*, *47*(W1), W5-W10. https://doi.org/10.1093/nar/gkz342

RStudio. (2020). *RStudio: Integrated Development for R. RStudio*. http://www.rstudio.com/.

Ruiz-Losada, M., Blom-Dahl, D., Córdoba, S., & Estella, C. (2018). Specification and Patterning of Drosophila Appendages. *J Dev Biol*, *6*(3). https://doi.org/10.3390/jdb6030017

Ryoo, H. D., Marty, T., Casares, F., Affolter, M., & Mann, R. S. (1999). Regulation of Hox target genes by a DNA bound Homothorax/Hox/Extradenticle complex.

1022 *Development*, *126*(22), 5137-5148. https://doi.org/10.1242/dev.126.22.5137
1023 Slattery, M., Riley, T., Liu, P., Abe, N., Gomez-Alcala, P., Dror, I., Zhou, T., Rohs, R.,
1024 Honig, B., Bussemaker, Harmen J., & Mann, Richard S. (2011). Cofactor
1025 Binding Evokes Latent Differences in DNA Binding Specificity between Hox
1026 Proteins. *Cell*, *147*(6), 1270-1282. https://doi.org/10.1016/j.cell.2011.10.053
1027 Struhl, G. (1982). Genes controlling segmental specification in the Drosophila thorax.
1028 *Proc Natl Acad Sci U S A*, *79*(23), 7380-7384.
1029 https://doi.org/10.1073/pnas.79.23.7380
1030 Timmermans, M., Roelofs, D., Mariën, J., & van Straalen, N. M. (2008). Revealing
1031 pancrustacean relationships: Phylogenetic analysis of ribosomal protein genes
1032 places Collembola (springtails) in a monophyletic Hexapoda and reinforces the
1033 discrepancy between mitochondrial and nuclear DNA markers. *BMC*
1034 *Evolutionary Biology*, *8*(1), 83. https://doi.org/10.1186/1471-2148-8-83
1035 Trapnell, C., Roberts, A., Goff, L., Pertea, G., Kim, D., Kelley, D. R., Pimentel, H.,
1036 Salzberg, S. L., Rinn, J. L., & Pachter, L. (2012). Differential gene and transcript
1037 expression analysis of RNA-seq experiments with TopHat and Cufflinks. *Nat*
1038 *Protoc*, *7*(3), 562-578. https://doi.org/10.1038/nprot.2012.016
1039 Tsuji, T., Sato, A., Hiratani, I., Taira, M., Saigo, K., & Kojima, T. (2000). Requirements
1040 of Lim1, a Drosophila LIM-homeobox gene, for normal leg and antennal
1041 development. *Development*, *127*(20), 4315-4323.
1042 https://doi.org/10.1242/dev.127.20.4315
1043 Tully, T., & Potapov, M. (2015). Intraspecific Phenotypic Variation and Morphological
1044 Divergence of Strains of Folsomia candida (Willem) (Collembola: Isotomidae),
1045 the "Standard" Test Springtaill. *PLoS One*, *10*(9), e0136047.
1046 https://doi.org/10.1371/journal.pone.0136047
1047 van Dam, S., Võsa, U., van der Graaf, A., Franke, L., & de Magalhães, J. P. (2018).
1048 Gene co-expression analysis for functional classification and gene-disease
1049 predictions. *Brief Bioinform*, *19*(4), 575-592.
1050 https://doi.org/10.1093/bib/bbw139
1051 van de Heuvel, M., Klingensmith, J., Perrimon, N., & Nusse, R. (1993). Cell patterning
1052 in the Drosophila segment: engrailed and wingless antigen distributions in
1053 segment polarity mutant embryos. *Development*, *119*(Supplement), 105-114.
1054 https://doi.org/10.1242/dev.119.Supplement.105
1055 van Straalen, N. M. (2021). Evolutionary terrestrialization scenarios for soil
1056 invertebrates. *Pedobiologia*, *87-88*, 150753.
1057 https://doi.org/https://doi.org/10.1016/j.pedobi.2021.150753
1058 Waterhouse, A. M., Procter, J. B., Martin, D. M. A., Clamp, M., & Barton, G. J. (2009).
1059 Jalview Version 2—a multiple sequence alignment editor and analysis
1060 workbench. *Bioinformatics*, *25*(9), 1189-1191.
1061 https://doi.org/10.1093/bioinformatics/btp033
1062 Weatherbee, S. D., & Carroll, S. B. (1999). Selector Genes and Limb Identity in
1063 Arthropods and Vertebrates. *Cell*, *97*(3), 283-286.

https://doi.org/10.1016/S0092-8674(00)80737-0

Wickham, H. (2016). *ggplot2: Elegant Graphics for Data Analysis*. https://ggplot2.tidyverse.org

Wu, J., & Cohen, S. M. (1999). Proximodistal axis formation in the Drosophila leg: subdivision into proximal and distal domains by Homothorax and Distal-less. *Development*, *126*(1), 109-117. https://doi.org/10.1242/dev.126.1.109

Yuzuki, D. (2015). *BGISEQ-500 debuts at the International Congress of Genomics 10*. In *Next Generation Technologist [online]* http://www.yuzuki.org/bgiseq-500-debut-at-the-international-congress-of-genomics-10